HIGH-PERFORMANCE LANDSAT/SPOT DUAL S-/X-BAND TELEMETRY TRACKING AND RECEIVING SYSTEM

BY: Bruce Bollermann - V.P. Technical
Roger Harshbarger - Electronics Engineer
Mark Haynie - Mechanical Engineer
Dr. Kailash Pande - Control Systems Engineer

SPACE DATA CORPORATION
1333 W. 21st Street
Tempe, Arizona 85282

ABSTRACT

A high-performance dual S/X-band telemetry tracking and receiving system has been developed to provide a low-cost earth station for receiving high-resolution data from current and future LANDSAT/Spot polar orbiting satellites. The antenna system consists of a dual S/X-band telemetry tracking feed in a Cassegrain configuration with a 10-meter parabolic reflector designed for 100 mph wind loading and 10 deg/sec^2 accelerations. The antenna system is mounted to a newly-developed elevation-over-azimuth tracking pedestal, which incorporates the latest technology in a dual brushless d.c. servo motor torque-biased drive train for each axis. This drive train provides an exceptionally wide dynamic range in trlcking velocities for very slow horizon tracking and very fast velocities for near-overhead passes. A microprocessor-based servo control system using the latest state variables feedback and adaptive control techniques is used to provide accurate tracking for both slow and fast rates. A 15-km satellite pass distance from overhead is used as a control system design criterion. For the narrow beamwidth X-band track this requires an acceleration error of less than 0.100 degree and an acceleration error constant of at least 90 sec^{-2}. The requirement for a high-performance servo system with the low structural resonances of a large antenna constitutes a difficult stability problem.

INTRODUCTION

Previous LANDSAT polar-orbiting satellites provided nominal resolution earth-scene data on L- and/or S-band downlinks. Medium diameter and medium performance tracking pedestals were adequate to track and recover data from these older satellites. However, the newer satellites, such as LANDSAT D and Spot, provide high-resolution data on X-band downlinks. Larger antennas on the order of ten meters in diameter and high-

performance tracking pedestals are required to track and recover data from these newer satellites. The larger size antenna is required for additional gain, and the resulting narrower beamwidth requires tighter tracking, ie, less off boresight tracking error. Therefore, many of the older LANDSAT receiving stations must be replaced to receive the new high-resolution data.

The LANDSAT S- and X-band receiving system recently developed (shown in Figure 1), includes a monopulse antenna system, an elevation-over-azimuth autotracking pedestal system, S- and X-band receiving equipment, a microprocessor-based control system, and a high-density tape recording system. Automated built-in test equipment is provided along with an S-band and X-band test target for systems testing and boresighting. The antenna and receiving systems are provided with a sufficient G/T for reliable reception of both S- and X-band LANDSAT and Spot satellite downlinks. The antenna consists of a 10-meter diameter reflector with a dual-frequency Cassegrain feed and subreflector assembly. Simultaneous reception of both S- and X-band downlinks is provided with this system. The antenna and pedestal are designed for survival in 100 mph winds and reliable satellite tracking in winds up to 40 mph. The microprocessor-based pedestal control system offers various selectable control modes including autotrack, manual position command, manual rate command, programmed acquisition mode, and programmed overhead drive mode. The system can be left unattended for automatic acquisition, track, and data reception. Automatic boresighting and systems testing can also be performed without operator intervention.

SYSTEM DESIGN AND PERFORMANCE

The system has been designed to track orbiting satellites at either S- or X-band and simultaneously receives data on both bands. Uninterrupted zenith reception in addition to automatic tracking acquisition is provided by microprocessor control of the antenna system.

The system receives and demodulates the data from three RF downlinks; ie, 2287.5 MHz S-band (RT), 2265.5 MHz S-band (MSS), and 8212.4 MHz.X-band (MSS, TM). These data are made available to a separate LANDSAT data processsing system for reduction into the final output form. The system block diagram is presented in Figure 2. The rf signals are preamplified and downconverted in the single-channel-monopulse antenna tracking feed. A separate tracking receiver located in the pedestal is used to detect the tracking error signals for the autotracking control system.

A microprocessor tracking control unit in the pedestal is used to control the elevation and azimuth axis servo drives. The console equipment includes both S- and X-band rf distribution and receiving systems. A console-located microprocessor pedestal control

unit communicates control commands to the pedestal tracking control unit and also controls various peripheral console equipment.

The major design and performance characteristics of the system are presented in Table 1.

A remotely-controlled dual S- and X-band test target is provided for automatic antenna boresighting and systems testing.

ANTENNA SYSTEM

The Cassegrain antenna system consists of a 10-meter paraboloidal reflector, a 1.2-meter diameter hyperboloidal subreflector, and a dual-band vertex-mounted singe-channel-monopulse tracking feed, as shown in Figure 3.

The S- and X-band telemetry and tracking feed block diagram is presented in Figure 4. The antenna gain at the comparator outputs is approximately 44.4 dBi for S-band (2.25 GHz) and 55.5 dBi for X-band (8.213 GHz). The antenna noise temperatures are estimated as 87.61°K for the S-band and 93.92°K for the X-band telemetry channels, and 162.2°K for the S-band and 191.7°K for the X-band tracking channels. Figure 5 illustrates the method used to calculate the X-band noise temperatures.

The reflector assembly consists of a reflector hub, 24 radial trusses and surface panels, 104 interchangeable intercostals, and required hardware. The reflector hub is 6 feet in diameter and 3 feet deep. It is fabricated as a reinforced aluminum cylinder with top and bottom flanges to interface with the radial trusses. Eight mounting pads on a 74.5-inch diameter bolt circle interface with the antenna support structure.

Twenty-four radial trusses are provided. The trusses attach to the top and bottom flange of the central hub and are interconnected by intercostal members to form an extremely rigid space frame. They provide support locations for the reflector surface panels, subreflector support spars, and locations for lifting the reflector during installation. The reflector surface consists of 24 pie-shaped panels that are fabricated on a precision production mold. Panel frames are constructed of aluminum extrusions with solid aluminum sheet reflecting surfaces which conform to the parabolic shape and attach to the frame with stainless rivets.

The feed assembly as indicated in Figure 6, consists of a 5-horn X-band cluster surrounded by a 4-horn S-band cluster. Monopulse comparators are used to form the aximuth and elevation difference channels for both bands. To obtain circular polarization, stepped-sceptum polarizers are used. These techniques are less lossy than dielectric vane polarizers and are thus preferred.

The S-band tracking feed consists of four diagonal horns in a diamond array configuration. They are of a pyramidal structure tapering to a square wave guide. Each diagonal horn aperture is truncated at two corners to make room for the X-band array and to provide a symmetrical response. This configuration reduces coupling between the S- and X-band apertures. The resulting isolation is greater than 50 dB. Waveguides transfer the signals to a monopulse comparator. The outputs of the comparator are the sum signal and the two difference (elevation and azimuth error) signals. The two difference outputs of the comparator are fed into a monopulse converter. Diodes are used for switching between channels. The output of the monopulse converter is amplified by a low-noise GaAs FET solid-state amplifier (LNA). The sum output is also amplified by a LNA. This output is divided into two equal parts in a power divider. One part is fed directly to the data channel downconverter. The other part is coupled to the amplified difference signal with phase correction. This creates the tracking segment of the sum channel. The S-band feed components, except the horns and polarizers, are located inside the hub.

A fixed-frequency downconverter located in the antenna hub converts the entire 2200 to 2300 MHz S-band to a 230 to 330 MHz intermediate frequency (IF). The downconverter preselection is a 100 MHz bandwidth filter centered at 2250 MHz and tailored for flat-group delay across the band. The input signal is mixed with the 1970 MHz local oscillator signal generated by a fixed-frequency microwave cavity oscillator phase-locked to a low-noise crystal oscillator. The output of the mixer is amplified by a wide-bandwidth, flat-group delay amplifier capable of driving in excess of 250 meters of coaxial cable. Isolators are used throughout the assembly to ensure good impedance matching between critical components. The downconverted S-band data signal is routed through low-loss coaxial cable to the control center where it is distributed via the rf distribution unit.

The X-band feed subassembly consists of an array of five circular horns, a sum horn, and 4 difference horns with dielectric lenses. The sum channel is amplified by a LNA and divided into two equal parts in a waveguide power divider. The data channel output passes directly to the data downconverter. A waveguide monopulse comparator mates with the four difference horns to form the ΔAZ and ΔEL error difference signals. The two difference signals pass through coaxial cable into a monopulse converter. This converter is a solid-state device which uses the scan commands from the tracking control unit (TCU) to commutate the rf tracking error signals. The modulated output is amplified by a LNA which passes through a waveguide phase-shifter and couples the tracking data to the sum signal by means of a directional coupler. The X-band feed block diagram is shown in Figure 7.

Two X-band downconverters for the data and tracking channels are located in the antenna hub. The data downconverter converts the LANDSAT 8.2125 GHz telemetry to a 375

MHz IF using a local oscillator frequency of 7.8375 GHz. It can also convert the Spot 8.253 GHz telemetry to a 375 MHz IF, using a switch-selectable 7.878 GHz local oscillator. Downconverted X-band data signals are routed via low-loss coaxial cable to the rf distribution unit located in the control center.

The entire S- and X-band feed assembly, along with associated waveguide, and rf electronics are housed in a weather tight aluminum cone which is bolted to the antenna hub. The hubcone assembly is pressure sealed by the radome and pressurized to 0.5 psig with dry nitrogen. A relief valve is provided at the top of the feed cone to allow purging the feed.

RECEIVER SYSTEM

The receiver system block diagram is shown in Figure 8. Both the S- and X-band receiving systems consist of the antenna system, preamplifier, power divider, downconverter, cable run, second power divider, isolation amplifier, and data and tracking receivers.

The tracking receiver located in the pedestal is a single-conversion superheterodyne P- band (250-320 MHz) type as indicated in Figure 9. Tuning and auto search are accomplished using a synthesized oscillator which is controlled by the microprocessor. Receiver outputs consist of signal strength, tuning, and AM tracking signals which are monitored by the TCU. The TCU passes the information to the Control Center and controls the receiver based on commands from the Control Center.

The downconverted S- and X-band telemetry signals, once routed through coaxial cable to the equipment room, are distributed via the rf distribution unit. The front panel of the distribution unit provides receiver inputs, and distribution amplifier inputs and outputs. Small quick-connect coaxial patch cables provide a compact and neat, but complete and functional, patch facility.

Two standard Microdyne Receivers with required plug-in modules are used as the S-band receivers and demodulators. These receivers take the S-band downconverted data and telemetry signals, detect and demodulate the PSK encoded data, and send it to the bit synchronizers. One system is used for the MSS data; the other provides the Real-time Telemetry Data (RT) which is used in processing MSS data. The MSS data and RT signals are routed from the receivers to two standard bit synchronizers. They lock onto the data stream, reforming a stable bit pattern and generating a synchronous clock signal. These data and clock signals are buffered and made available at the data distribution panel.

A block diagram of the LANDSAT X-band Data Receiver/Demodulator is presented in Figure 10. In the-demodulator portion, the IF signal plus noise is bandpass filtered, AGC amplified, and then routed to the demodulator. A voltage-controlled oscillator and multiplier assembly provides a 0° and 90° phase local oscillator signal to the demodulator. It is phase-locked to the incident IF. In the demodulator, in-phase and quadrature demodulation occurs. The noisy baseband outputs are the inputs to the 84.903 Mbps signal conditioner, signal plus noise is optimally filtered and then state estimated. The matched filter output is also routed to the bit synchronizer where an even order nonlinearity produces a bit rate spectral component. A phase-lock loop is locked to this spectral component with the VCO output being both an external output and control for state estimation in the signal conditioner. On the Q channel, similar processing occurs with the 15.062 Mbps data stream plus noise.

In the input processor, the IF signal plus noise is wideband bandpass filtered to eliminate spurious signals and then variable gain amplified. The envelope detection for automatic gain control is accomplished in the carrier regeneration circuitry where filtering is narrower and thus signal-to-noise higher. Noncoherent AGC makes output level independent of phase noise. The variable gain amplifier output is power divided and sent to the carrier regeneration circuitry and to the coherent demodulator.

In the demodulator, the IF S + N from the input processor is power divided and routed to the phase detectors. The L ports of these detectors are driven by quadrature components from the local oscillator (LO). The LO reference input is split into quadrature components by a quadrature hybrid. The hybrid outputs drive the phase detector L ports. Both the I and Q baseband outputs are filtered by constant resistance low-pass filters to remove sum frequencies and LO feedthrough. The I output connects to the 84.903 Mbps bit synchronizer while the Q output connects to the 15.062 Mbps bit synchronizer.

The bit synchronizer baseband S + N input is optimally filtered by the matched filter which is sliding integral approximation. The outputs y(t) of the matched filter are the input to the decision unit and also to phase-lock loop. In the decision unit, a comparison to a reference level at the end of each period and a state estimate, for each bit is made. The timing for the decision unit is provided by the synchronizer portion of the bit sync. The phase-locked loop is filtered to remove data variations. Outputs from the filter are routed to the bit decision circuitry and to the differential decoder. Data from the bit decision circuitry also goes to the differential decoder. The differential decoder resolves and removes any remaining ambiguities in the data and clock signals.

PEDESTAL

An outline drawing of the LANDSAT Model 896 Autotracking Pedestal is shown in Figure 11. This pedestal is a two-axis elevation-over-azimuth, servo motor gear-driven pedestal, designed to support and control parabolic reflectors up to 12 meters in diameter under high wind and drive acceleration conditions. It has been designed for stiffness and high resonant frequencies which are necessary for autotracking applications. The dish and pedestal are tightly coupled through the use of two large-diameter integral gears with precision cross roller bearings mounted to the elevation turntable, which in turn, mounts directly to a rigid antenna support structure. This structure provides the interface between the pedestal and the antenna.

Major features of the pedestal are:

- Dual Torque-Biased brushless DC Servo Motor Drive Trains
- High-resolution Brushless Tachometers
- Machined Steel Billets for Gear Train Housings
- Eccentric Backlash Adjustments
- Large Cross Section Cross Roller Bearings

The drive trains provide high torque to inertia ratios, low weight, low maintenance, and an exceptionally wide dynamic range for low-speed tracking over the horizon and high-speed tracking during an overpass.

The pedestal is constructed of heavy-section steel weldments with continuous welds inside and out to provide stiffness and seal the interior from water and dust. All components inside the pedestal can be reached through large access doors which are hinged for convenience. These doors may also be removed completely, if desired, to permit work to be done. The elevation doors are equipped with gas springs which hold the door up and out of the way of the operator when open.

Each axis is equipped with fail-safe electromechanical brakes and stow locks for protection. The elevation stow lock is easily accessible from the ladder on the outside. The azimuth stow lock is accessed from the inside of the pedestal. These stow locks are used to prevent gear train damage when the dish is subjected to excessive high wind loading.

Each axis is equipped with two brushless dc servo motors. These brushless motors have an excellent field record and were chosen because of their ease of maintenance (no brushes or slip rings to be replaced), and their superior performance over a large dynamic range. The use of rare earth magnets in the motors gives a greater torque to inertia ratio and faster accelerations than comparable dc servo motors. The unique stator design

virtually eliminates cogging or torque ripple thus allowing smooth tracking even at very low speeds. Due to the absence of brushes in these motors, the top speed is substantially higher than comparable dc servo motor top speeds; thus, allowing faster tracking speeds.

Each motor is equipped with electromechanical fail-safe brakes which have manual hand release levers, a tachometer for rate loop damping of the servo loop, and hand cranking provisions to allow movement of the dish during power failures.

A dual drive system is used in a torque bias configuration for each axis. The dual drive includes two separate motors and gear boxes for each axis. Using a torque bias configuration helps to eliminate backlash problems at low speeds. The gear boxes are planetary-reduction gear assemblies. By using planetary gears, a very stiff gear train can be packaged in a relatively small volume. Each planetary gear box drives directly on the main drive gear. Using this arrangement, it is possible to get twice the torque capacity from the same integral gear bearing as is possible with a single drive configuration. All four motors in the pedestal are completely interchangeable as are many of the planetary gear reducer parts between the azimuth and elevation axes, making them less expensive to produce and maintain. The azimuth gear reduction ratio is 978:1 and the elevation gear reduction ratio is 1676:1. Each motor is capable of providing 30 ft-lb of torque.

The pedestal velocity and acceleration rates are 26°/sec and $10^\circ/\text{sec}^2$ for azimuth and 5°/sec and $10^\circ/\text{sec}^2$ for elevation. These rates will be limited in manual operation modes for operator and equipment safety reasons.

The azimuth turntable is supported by a 48-inch precision cross roller integral gear bearing. The turntable has a 10-inch hole for cable runs or a rotary joint. The azimuth axis is equipped with primary and secondary limit switches to provide protection to the cable wrap along with software limits.

The elevation drive has two 36-inch precision cross roller integral gear bearings mounted in a vertical position. These bearings are spaced 56 inches apart to allow room for cable runs, electronics, motors, gear boxes, and encoders. A 10-inch hole is provided for cable runs or a rotary joint. The elevation axis is equipped with primary and secondary limit switches. The primary switches will provide a direction limit to the servo system, the secondary switch will remove power from the servo system. In the event that the limit switches would fail, the elevation axis is equipped with mechanical limits which will stop rotation and prevent damage to the dish.

The antenna support structure or load arms is a weldment made of heavy steel plate which closely couples the dish and counterweights to the pedestal providing an extremely stiff interface so that the drive system stiffness is transmitted to the antenna. By closely

coupling the dish and pedestal, lower inertias are realized and minimum loads are induced into the antenna support structure which degrades boresight accuracy under dynamic conditions.

Position feedback for the pedestal is provided by absolute optical encoders. The azimuth unit is a 16-turn 16-bit encoder which has an anti-backlash gear mounted to its shaft and is driven directly by the azimuth output axis bull gear. The elevation encoder is a single turn 15-bit encoder which is mounted directly to an elevation turntable. The encoders provide least significant bits of 0.0144 degree and 0.011 degree in the azimuth and elevation axes, respectively.

Care has been taken throughout the pedestal to protect it from corrosion. The integral gear bearings are plated with a thin dense chromium plating and are equipped with external seals. All hardware is zinc or cadmium plated, and all steel surfaces are painted with two-part epoxy paint that stands up to weather well and does not stain when it comes in contact with bearing grease.

An automatic pedestal tilt mechanism is provided for satellite tracks which come directly overhead. Coordinate transformations are automated in the microprocessor control units to correct the encoder angles for the off-vertical tilt angle.

The standard riser base is a 15-foot truncated cone with a 10-foot base diameter made of rolled steel sections welded together. This riser provides an excellent base to mount the pedestal on due to its stiffness and capability to house the electronics required for tracking. A full-size door is provided in the base to easily access the electronics and the azimuth pedestal housing. A swing-out ladder is provided inside the riser to allow access to the pedestal azimuth unit. There is also a work platform provided which allows work to be carried out comfortably on the azimuth drive system and electronics. A riser extension section can be provided in the length required if there is a need to elevate the dish to a height greater than the height given by the pedestal on the standard riser.

All servo power and electronics, along with power supplies for the feed, are housed in the riser in enclosures which provide protection from moisture and dust. The electronics are easily accessible for troubleshooting and repair. The feed pressurization bottle and regulator are also housed in the riser for convenience and protection.

The pedestal and riser base are provided with environmental control. They can be provided with heating and/or air conditioning which are automatically controlled. The interior of the riser base is coated with a hard surface foam insulation to reduce heating or cooling loads. The heating and cooling systems are closed systems. Each consists of two separate units which act as backup for the other unit. An electromechanical timer

automatically switches power from one system to the other every 12 hours to wear the units evenly. The switching also ensures that heating or cooling will occur every 12 hours if one system becomes inoperative. The air conditioning system is controlled by temperature and humidity. The humidity control ensures there will not be moisture buildup on the electronics inside the riser base.

CONTROL SYSTEM

The LANDSAT tracking and pedestal control system provides various antenna positioning control modes through microprocessor software programming selections. Provisions are made for manual rate command, manual position command, automatic acquisition scan modes, and various autotracking modes which include both Type 1 and 2 servo systems with various gains and servo bandwidths.

The autotrack servo control systems consists of a microprocessor servo control unit, servo power amplifiers, dc servo motors, gear trains, a tachometer for each tracking axis, and a single-channel-monopulse tracking feed and associated electronics used to generate the tracking error signals.

The position command servo system utilizes the same servo system hardware components as for the autotrack system with the replacement of the antenna pattern and rf electronics error signals by the pedestal angle encoder feedback signals. The input command angles can be selected by the operator at the console or can be a preprogrammed set of acquisition scan angles generated by the microprocessor system control unit.

The rate command system consists of the same basic servo component hardware with the feedback signal generated by the the pedestal velocity measuring tachometers rather than the encoders. In general, the rate command inputs will be generated by the operator at the console by means of a joystick. Computer-generated rate commands will also be used as required.

The Pedestal Control Unit, located in the control center, has a plasma display and detached keyboard and is used to provide communications with the microprocessor controller in the pedestal.

The major functions of the Pedestal Control Unit are:

- Provide pedestal status information to operator.
- Entry of orbital parameters.
- Calculate satellite position versus time.
- Send position information to Tracker Control Unit for satellite acquisition.

- Display system diagnostics information.
- Operator inputs for pedestal set-up.

A simplified block diagram of the autotracking control system is shown in Figure 12. The performance of this system is far more critical than the other servo systems since the off-boresight pointing error of the antenna must be maintained within 0.1 degree during all periods of the autotrack; otherwise, a break in track will occur. The system is designed to maintain autotrack for satellite passes as close as 15 km from directly overhead. The timewise profiles of azimuth angle tracking for this 15 km overpass are shown in Figures 13 through 15. These profiles indicate that the antenna must be rapidly slewed in azimuth angle by essentially 180° over the short time period of about 8 seconds. The maximum velocity exceedes 25 deg/sec during the overpass and acceleration reaches about 8 deg/sec^2 on both sides. To maintain autotrack during this period the acceleration error coefficient must be greater than 90 sec^{-2}.

CONTROL SYSTEM ANALYSIS

A mathematical model accounting for the compliance in the drive train connecting the motors to the antenna load is derived from the resulting transfer functions and are presented in the mathematical block diagram in Figure 16. The transfer function relating the motor speed W_m to the motor torque T_m exhibits a pair of complex zeros, a pair of complex poles and one real pole. The complex poles and zeros are a consequence of the compliance in the drive shaft. The next two blocks represent the dynamic relationship between the motor speed W_m and the antenna angular motion θ_o.

The motor rate is sensed by a tachometer and feedback to form the rate loop stabilizing the system. The position loop is completed by the rf sensing of the off-boresight angle representing the position error signal e.

The controller consists of a proportional plus integral controller. The integral action is added to provide a good tracking performance in the presence of fast changing tracking command θ_i. The controller is implemented in the microprocessor using a backward difference approximation of the state-variable model of the controller. The rate feedback is also implemented digitally through the microprocessor control unit. The resulting actuating signal is finally converted to an analog form and represents the input to the power amplifier.

The control system is required to achieve the basic performance requirements of a good transient response and the ability to track the most severe tracking command with a log error of less than about 0.1°. This must be achieved through a judicious selection of the

rate feedback gain K_D (or $K_R = K_{AD}\, K_{TG}\, K_D$), the system forward gain, K, and the zero location A. Presently, the classical root locus method is used to arrive at a suitable design.

Figure 17 shows the root locus plot for the rate feedback loop where K_R represents the variable gain. The choice of K_R determines the closed-loop poles for the rate loop which eventually appear as the open-loop poles for the position loop. A large value of K_R would result in close-loop poles for the rate loop well to the left of the imaginary axis, a desirable feature in itself. However, the acceleration error constant for the overall system is given by:

$$K_a = \frac{KK_mC_2A}{n\,(J_md_o + K_mK_RC_2)} \quad \frac{KA}{nK_R} \qquad (1)$$

A large K_R would thus reduce K_a, and hence, the ability to track a fast changing tracking command. Its effect may be offset to some extent by increasing the gain, K, but this may create problems in selecting suitable closed-loop poles for the overall system. Consequently, a compromise value of $K_R = 20$ was chosen which gave sufficiently damped closed-loop poles for the rate loop as indicated in the figure.

The position loop exhibits different root locus patterns depending on the choice of the controller zero location A. As seen from Eqn.(l), smaller values of A would require higher K values to obtain the same acceleration error constant.

Alternatively, a smaller value of A may be selected to permit the choice of K so as to yield well damped ($\zeta \simeq 0.7$) closed loop poles for the system. Simultaneously, the error constant may be restored to the desired value through the use of a log compensator in cascade. This approach was tried but failed to provide the required tracking for a 15 km pass. Apparently, this is because the tracking command consists of a fast varying acceleration and is thus much more severe than the classical constant acceleration input on which the error constant K_a is based. However, a consideration of K_a would still provide some guidance during the analytical design.

A higher value of A = 4 was then selected and the resulting root locus plot for the position loop is shown in Figure 18. An error constant value of approximately $K_a = 100$ is achieved with a gain $K = 5 \times 10^5$ and results in the closed-loop poles indicated in the figure. The dominant closed-loop poles exhibit a damping ratio $\zeta \simeq 0.23$ and some response from the real pole near the open-loop zero may be expected. This design was found capable of tracking the 15 km miss distance quite well. It appears that a system with a relatively lighter closed-loop damping ratio would track fast changing inputs with a smaller log error.

SYSTEM SIMULATION AND RESPONSE

A computer program has been developed to simulate the performance of the autotrack control system. The program utilizes a sixth order state variable model for the rate and position loop dynamics, and integrates these numerically using a fourth order Runge-Kutta algorithm. The controller is modeled by a difference equation representing the microprocessor function and sampling effects. In addition to the linear model discussed earlier, the simulation accounts for nonlinear effects such as amplifier saturation and coulomb friction.

A typical response to a step input command of 0.1°, representing acquisition of the satellite by the tracker, is shown in Figure 4. The response indicates a settling time of approximately 1.5 sec. which appears adequate.

The tracking performance of the system was evaluated by providing the command input shown in Figure 19 to the simulation program. The control system performance was found quite satisfactory and resulted in the log error profile presented in Figure 20. As anticipated, the azimuth angle logs the A accelerating input until the time of closest pass and then leads it as the tracking input decelerates. The maximum tracking log error may be further reduced by increasing the system gain, K. The simulation experience indicates that a sampling rate of about 100 Hz is adequate for stable system behavior.

Present efforts are directed to a state variables design which includes current feedback and optimizing algorithms to improve upon the performance reported herein.

The angular noise error or jitter in a single channel pseudo-monopulse system is primarily a function of the carrier signal-to-noise ratio and the servo bandwidth. As the signal-to-noise ratio becomes poorer, or the servo bandwidth is widened, the tracking angle noise errors increase. Fortunately, distant tracking produces low acceleration requirements for which narrow servo bandwidths can be used. We are therefore considering a form of adaptive control in which the system gain constants are changed with the rf carrier signal-to-noise ratio to reduce the angular noise error (jitter) for distant tracking.

ACKNOWLEDGMENT

SDC has delivered the first LANDSAT Receiving Station to the Government of Indonesia, National Institute of Aeronautics and Space at the LAPAN Facility.

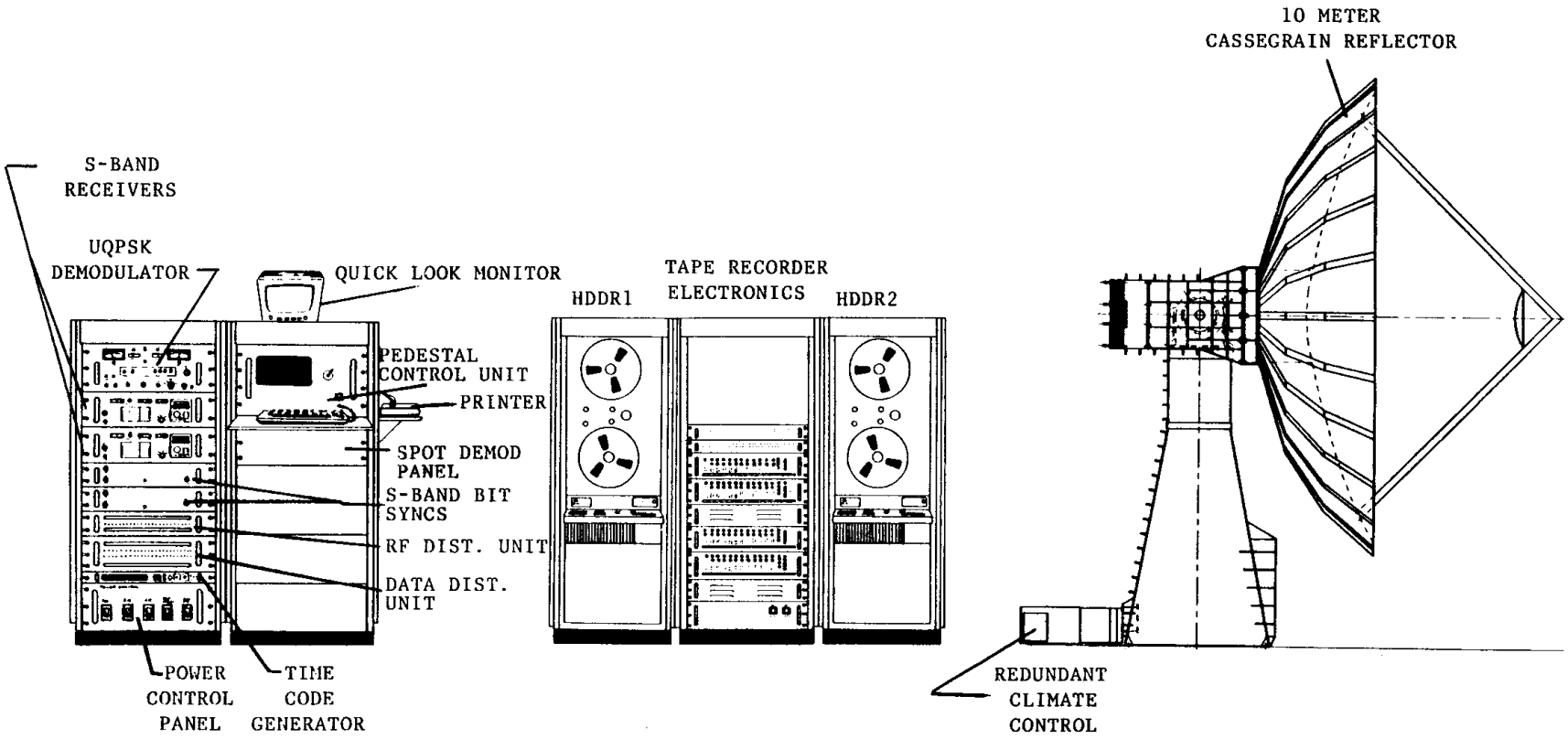

Figure 1. LANDSAT Receiving Station

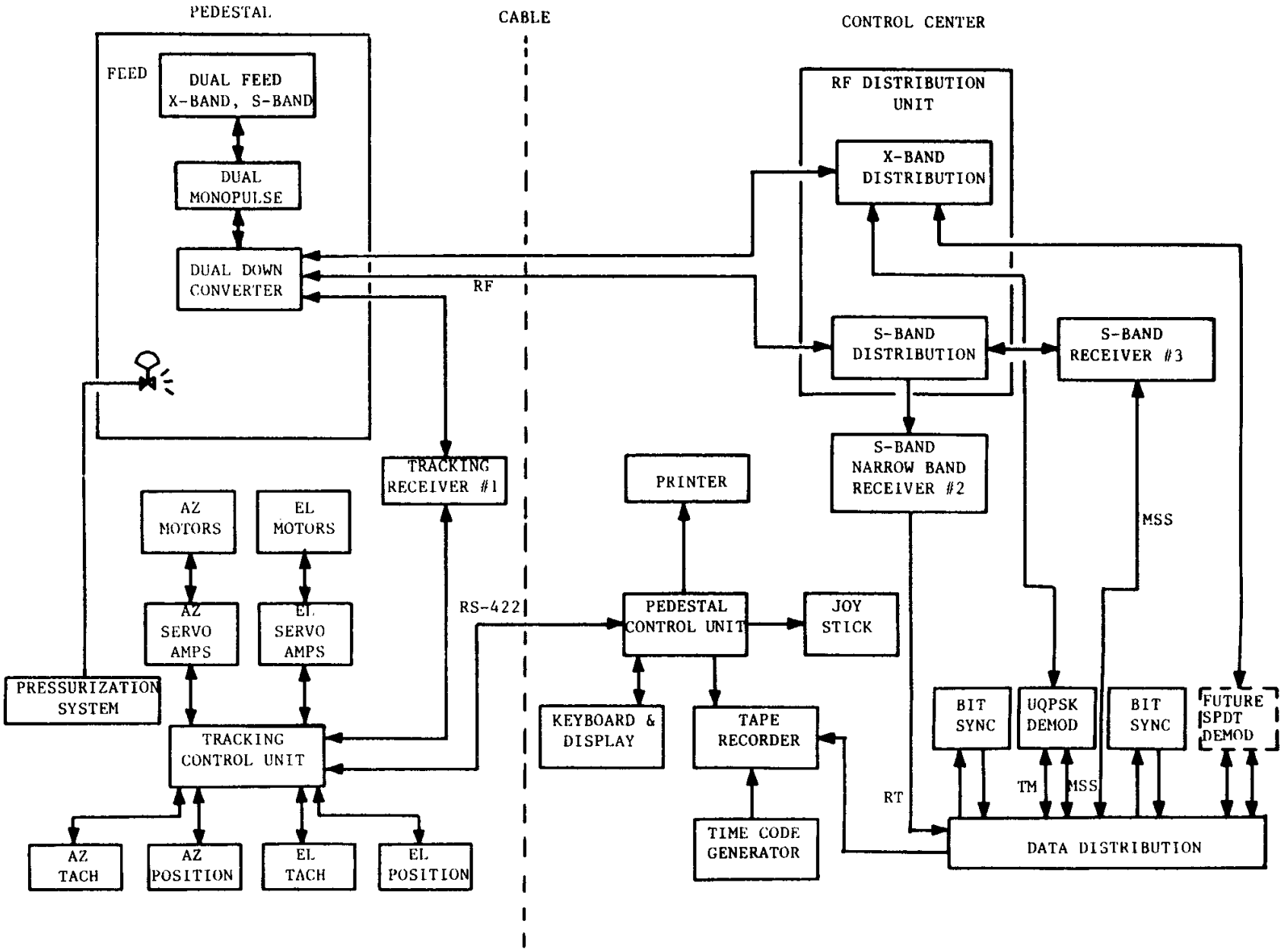

Figure 2. System Block Diagram

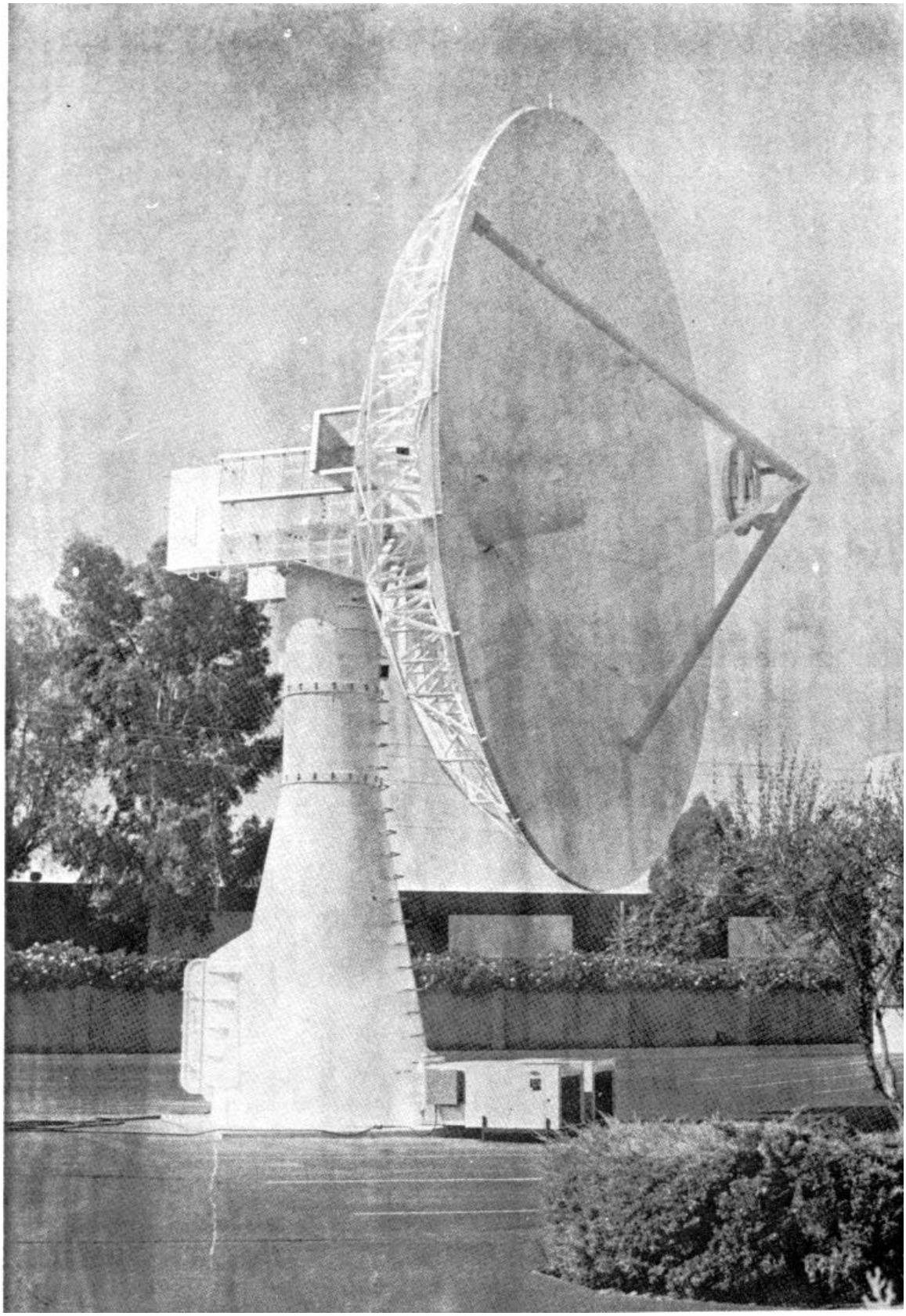

Figure 3. Landsat Tracking and Receiving Antenna and Pedestal.

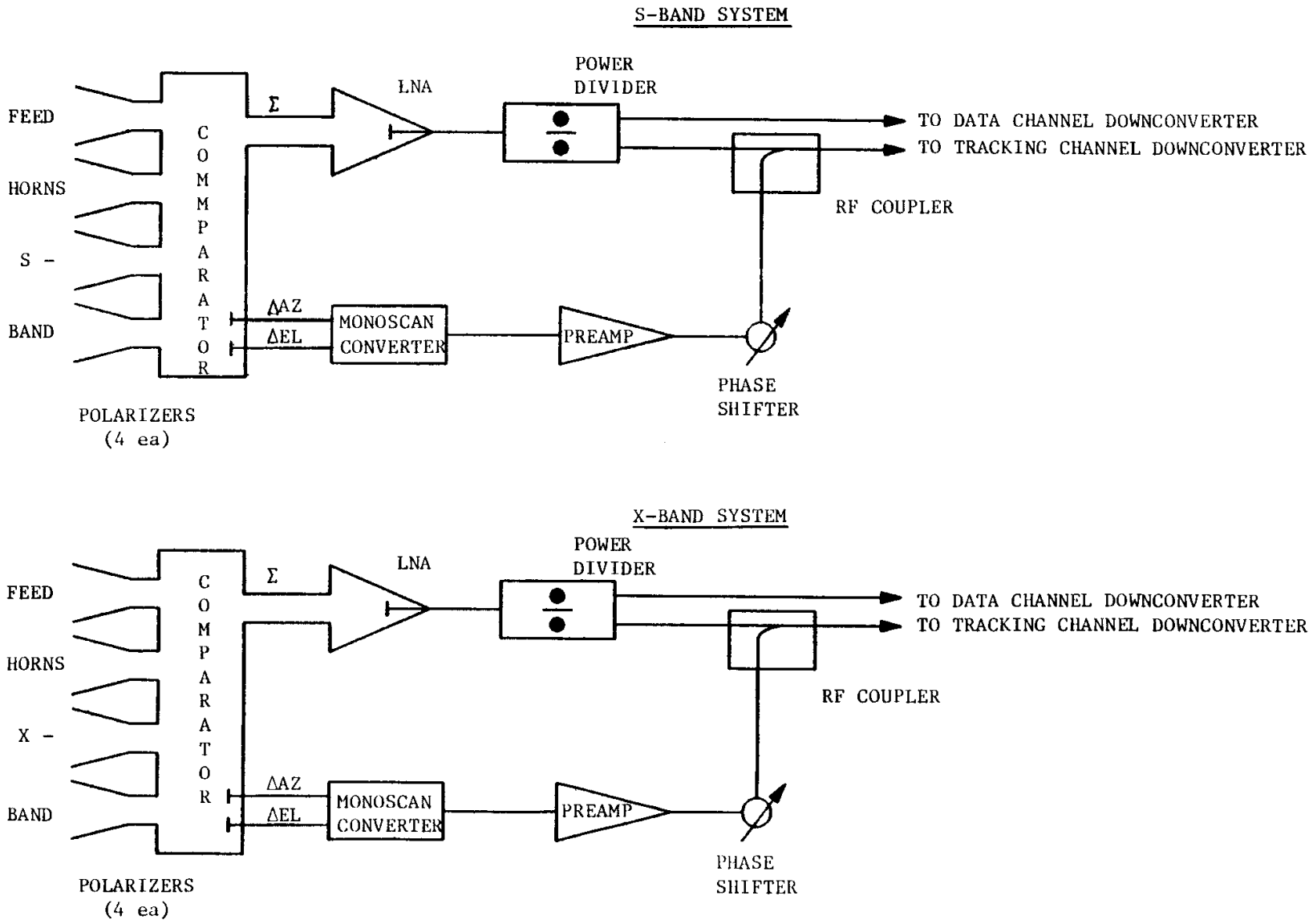

Figure 4. S-Band & X-Band Telemetry & Tracking Feed Block Diagram

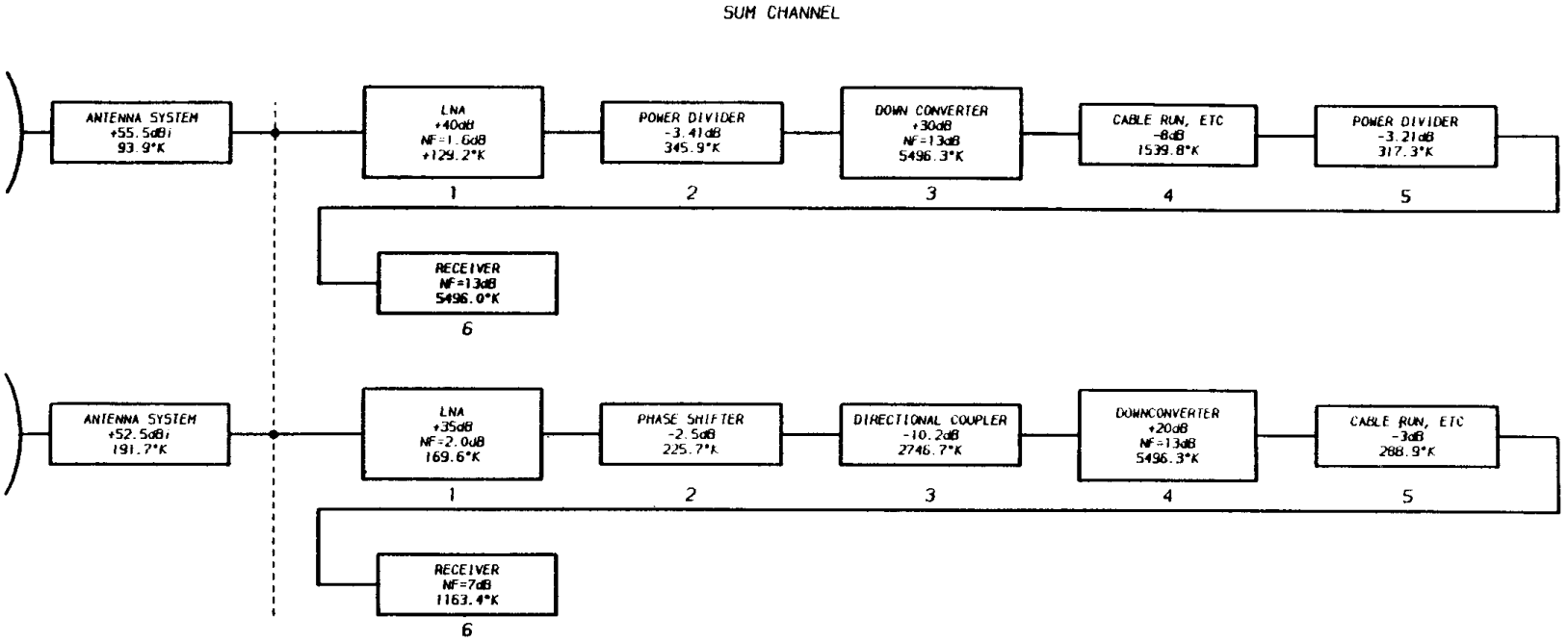

$$T_R = T_1 + \frac{T_2}{G_1} + \frac{T_3}{G_1 G_2} + \frac{T_4}{G_1 G_2 G_3} + \frac{T_5}{G_1 G_2 G_3 G_4} + \frac{T_6}{G_1 G_2 G_3 G_4 G_5}$$

$$T_{RS} = T_A + T_R$$

$$G/T = \frac{G_{ANT}}{T_{RS}}$$

	SUM CHANNEL	TRACKER CHANNEL
T_A	93.9°K	191.7°K
T_R	130.5°K	203.8°K
T_{RS}	224.4°K	395.5°K
G_A	55.5db	52.5dBi
NOISE FIGURE	2.49dB	3.74dB
G/T	32.0dB/°K	26.5dB/°K

Figure 5. X-Band Receiving Systems Noise Temperatures (8.21 GHZ, 5° Elevation, 290°K Ambient Temperature)

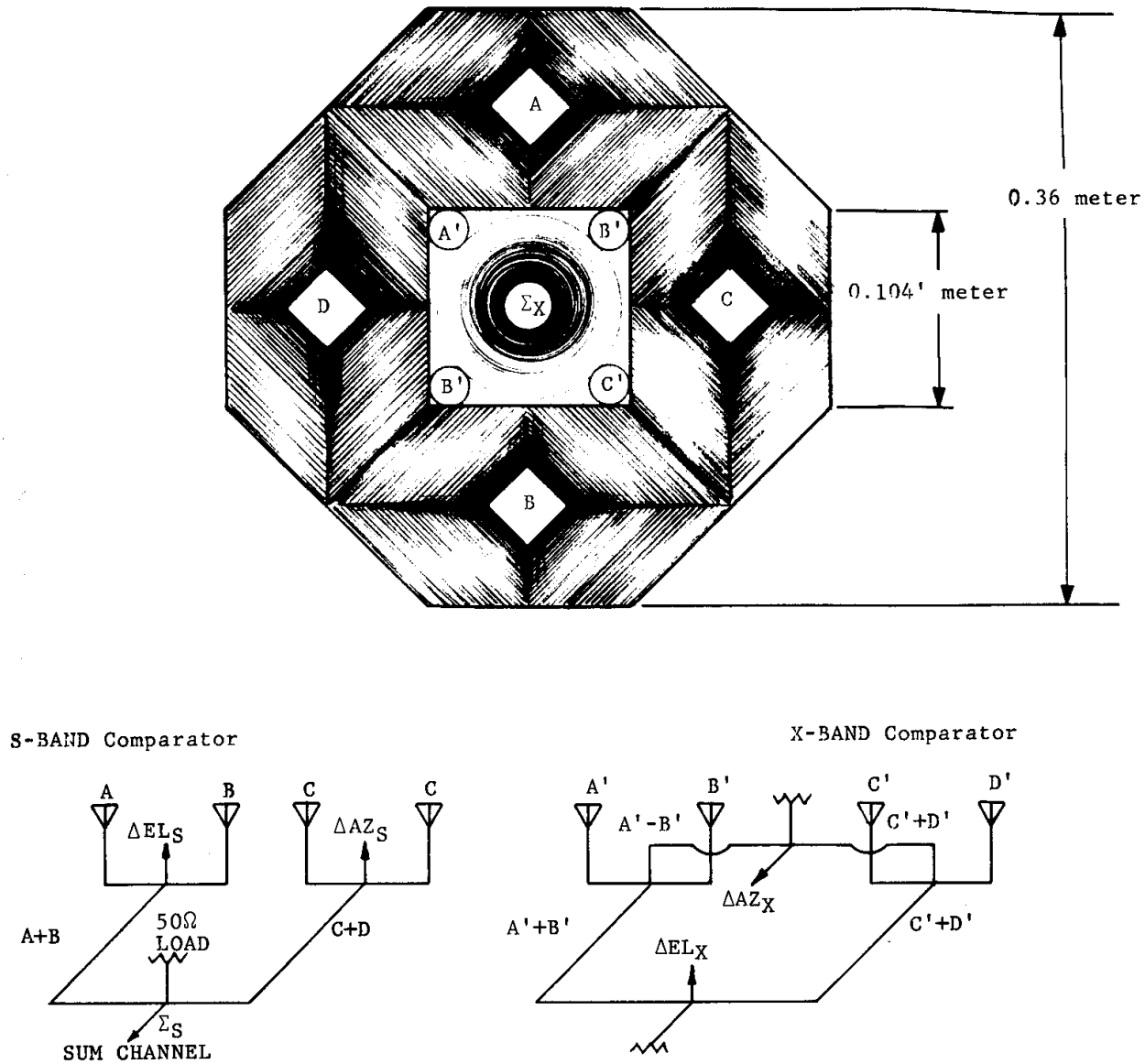

Figure 6. Dual Band Feed Horns and Waveguide Comparators for Sum ( ) and Difference (Δ) Channels

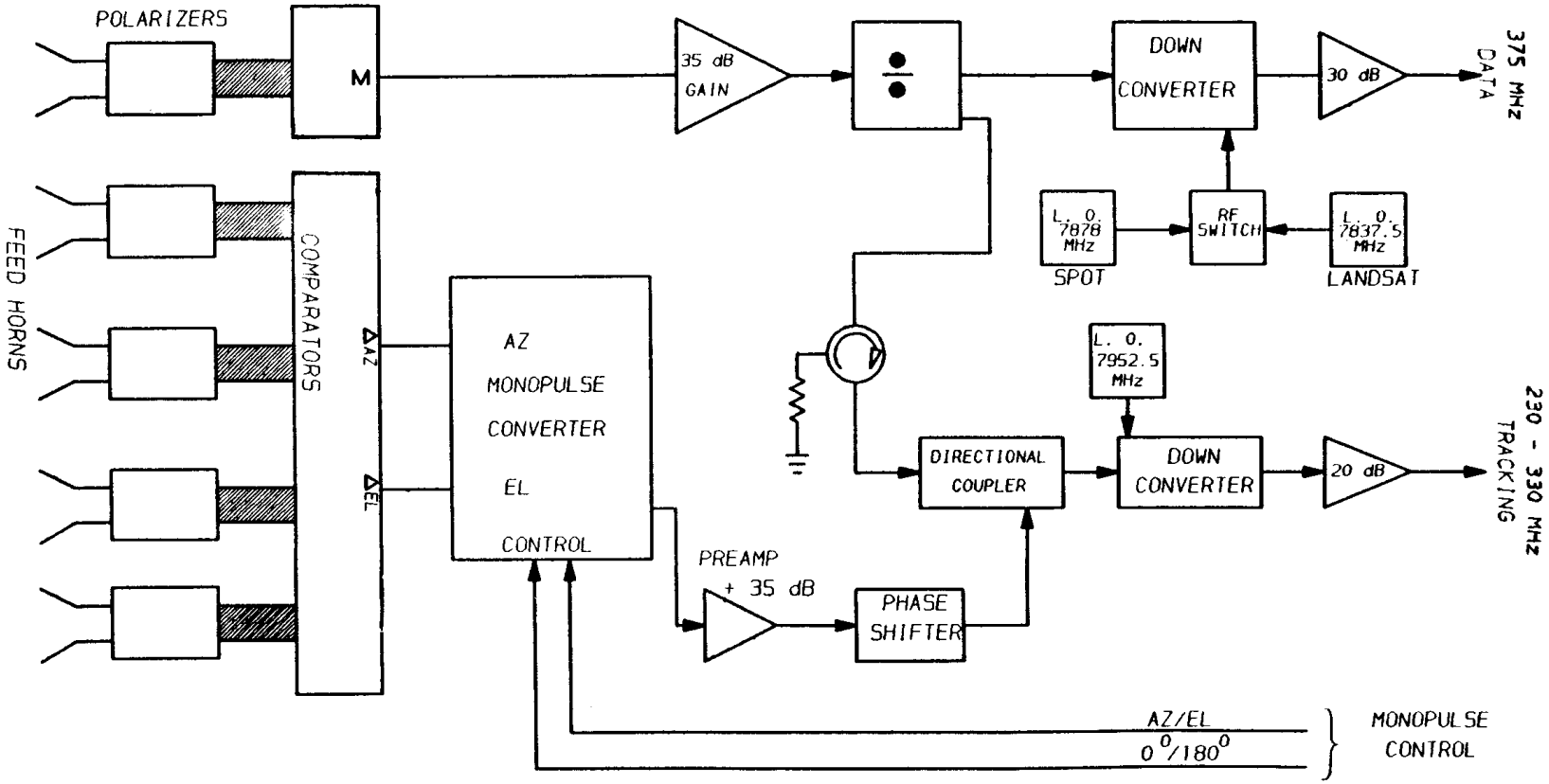

Figure 7. X-Band Feed Block Diagram

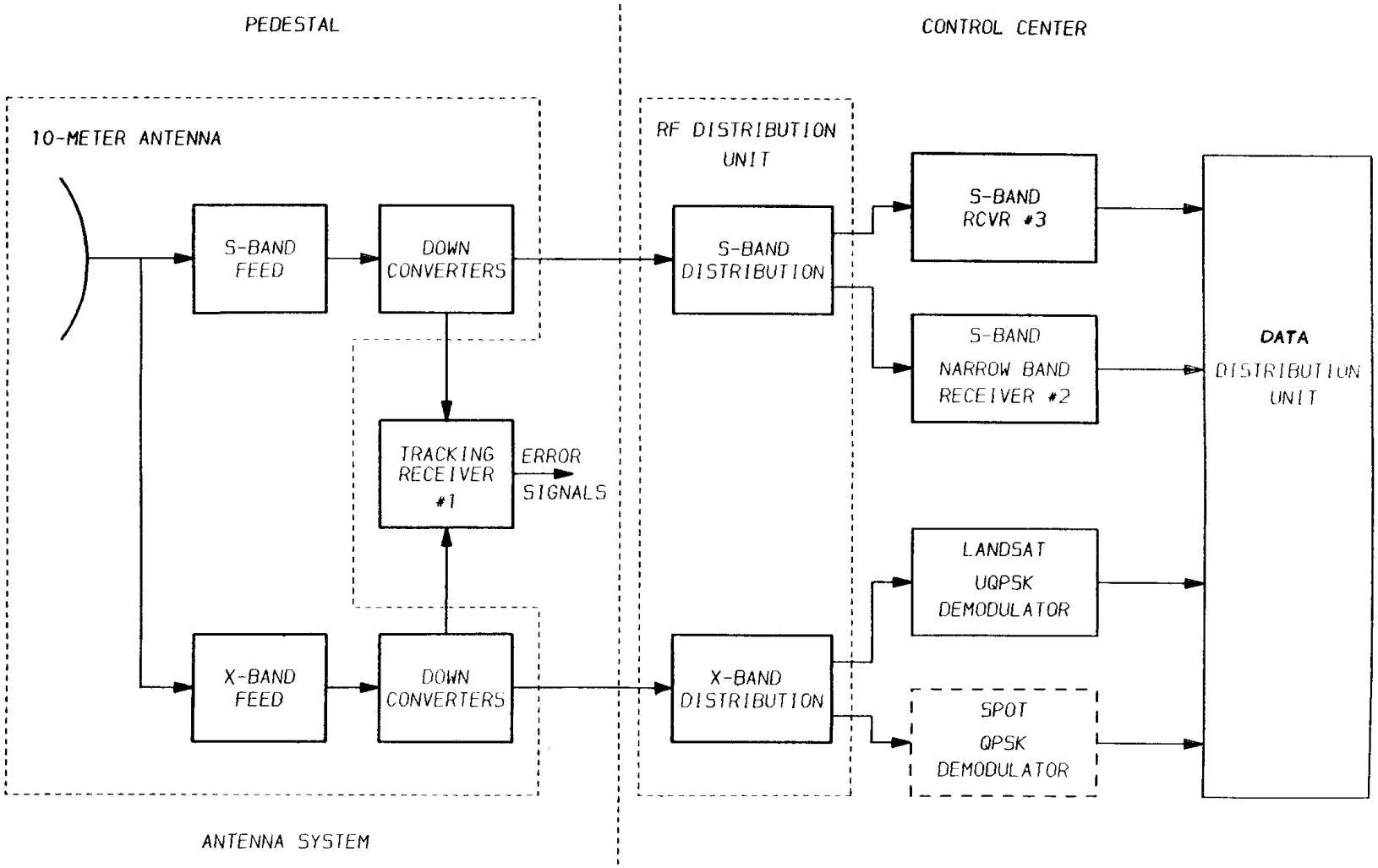

Figure 8. Receiver System Block Diagram

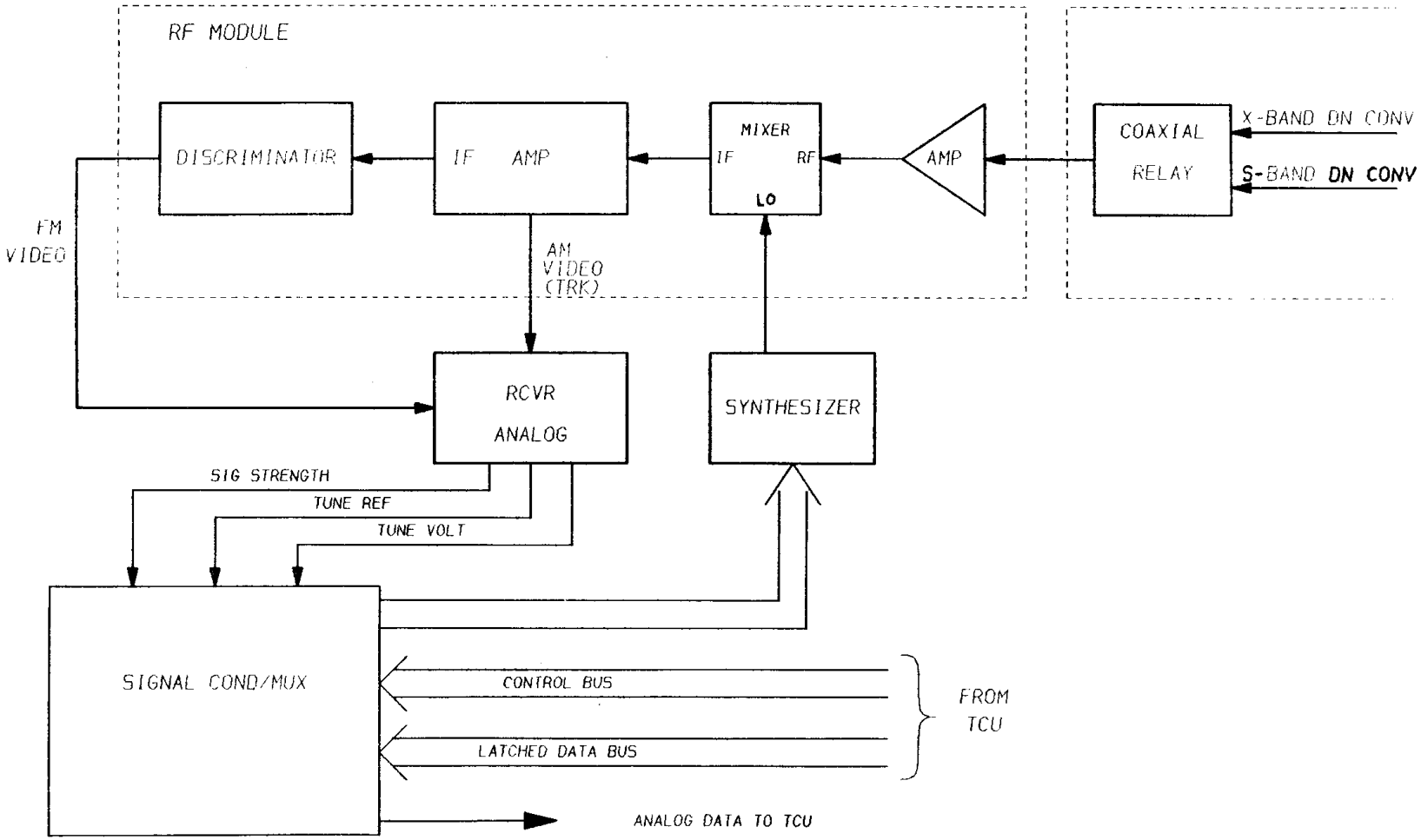

Figure 9. Tracking Receiver Block Diagram

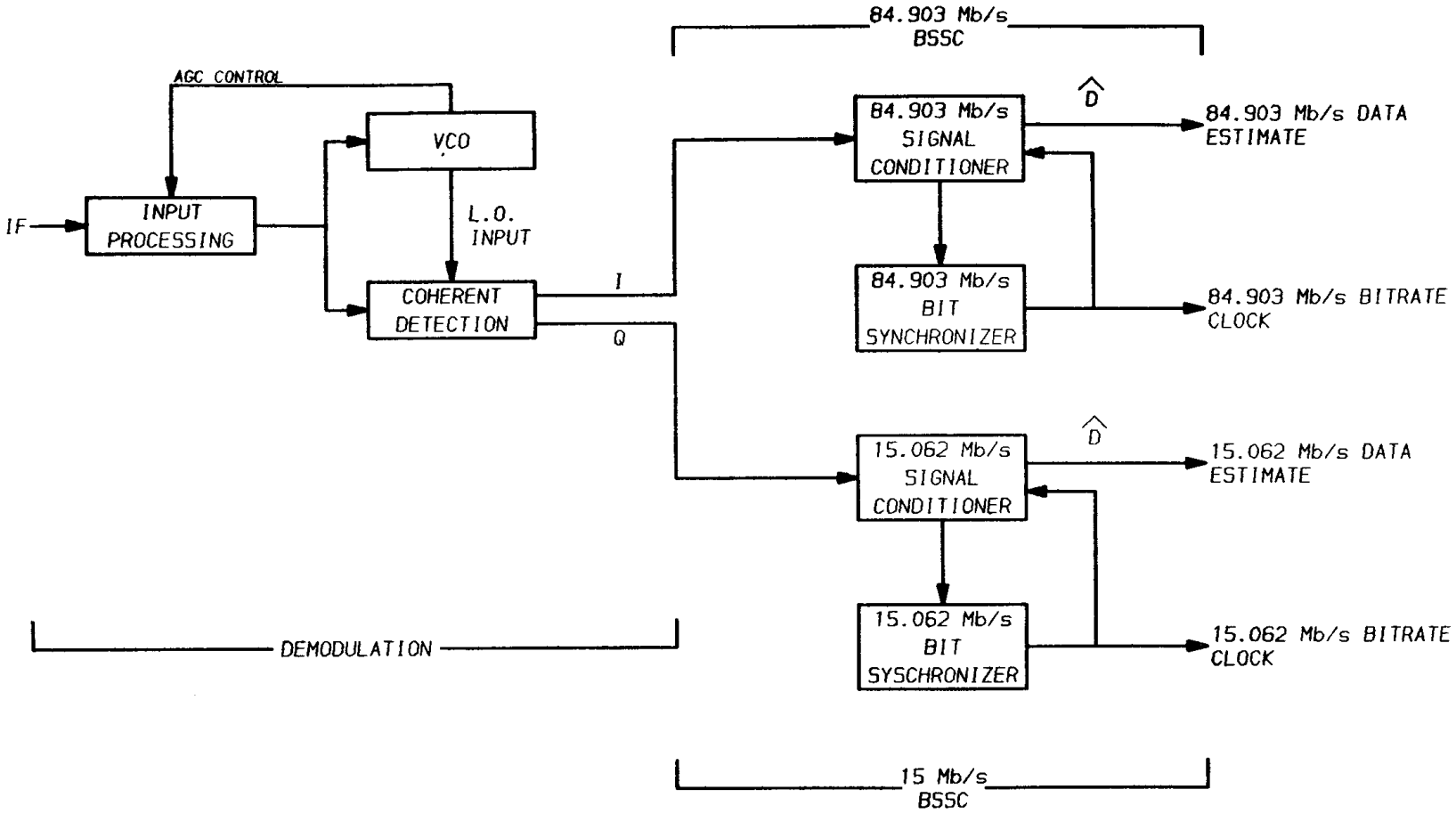

Figure 10. LANDSAT X-Band Data Receiver/Demodulator

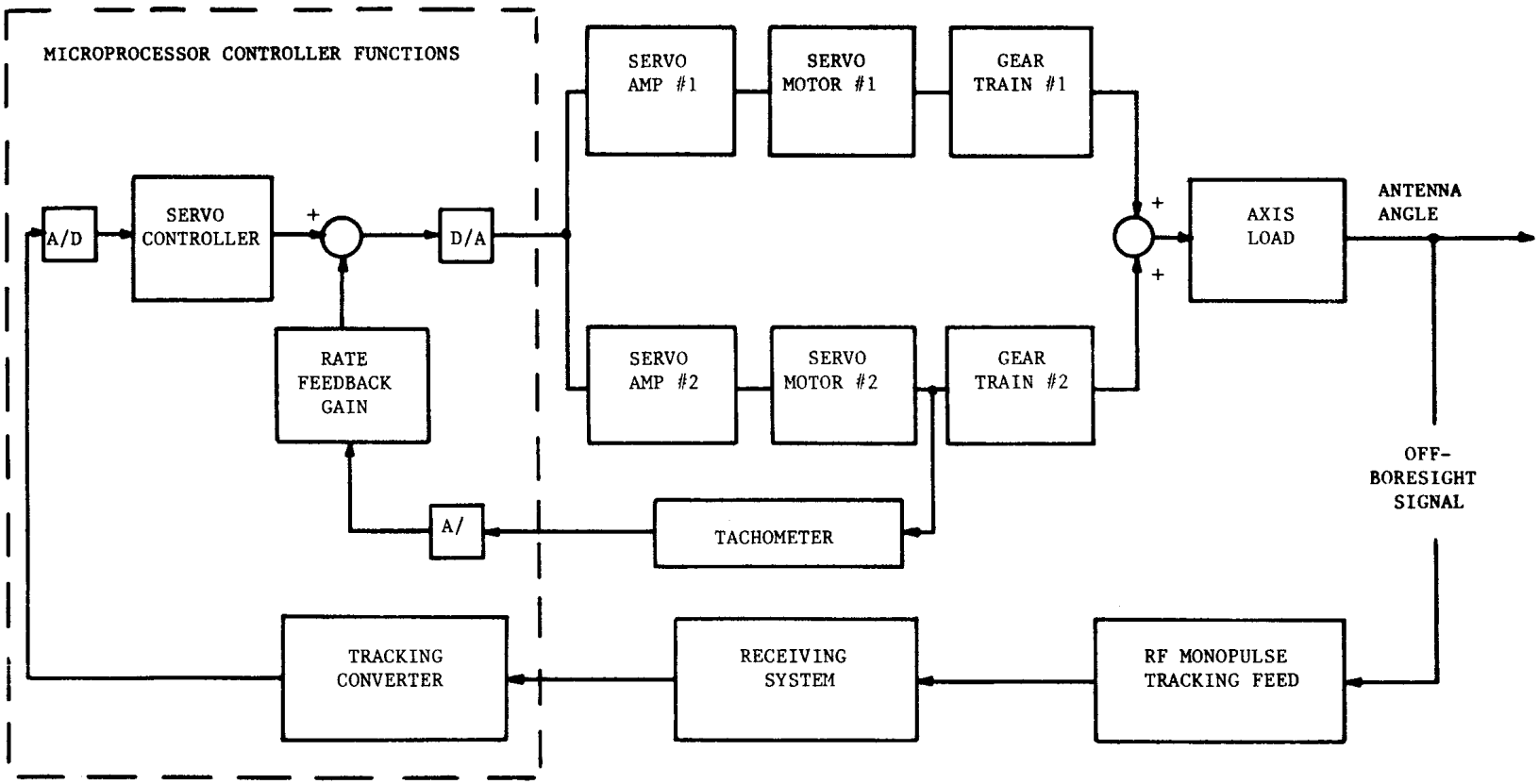

Figure 11. Autotracking Control System-Simplified Block Diagram for One Axis

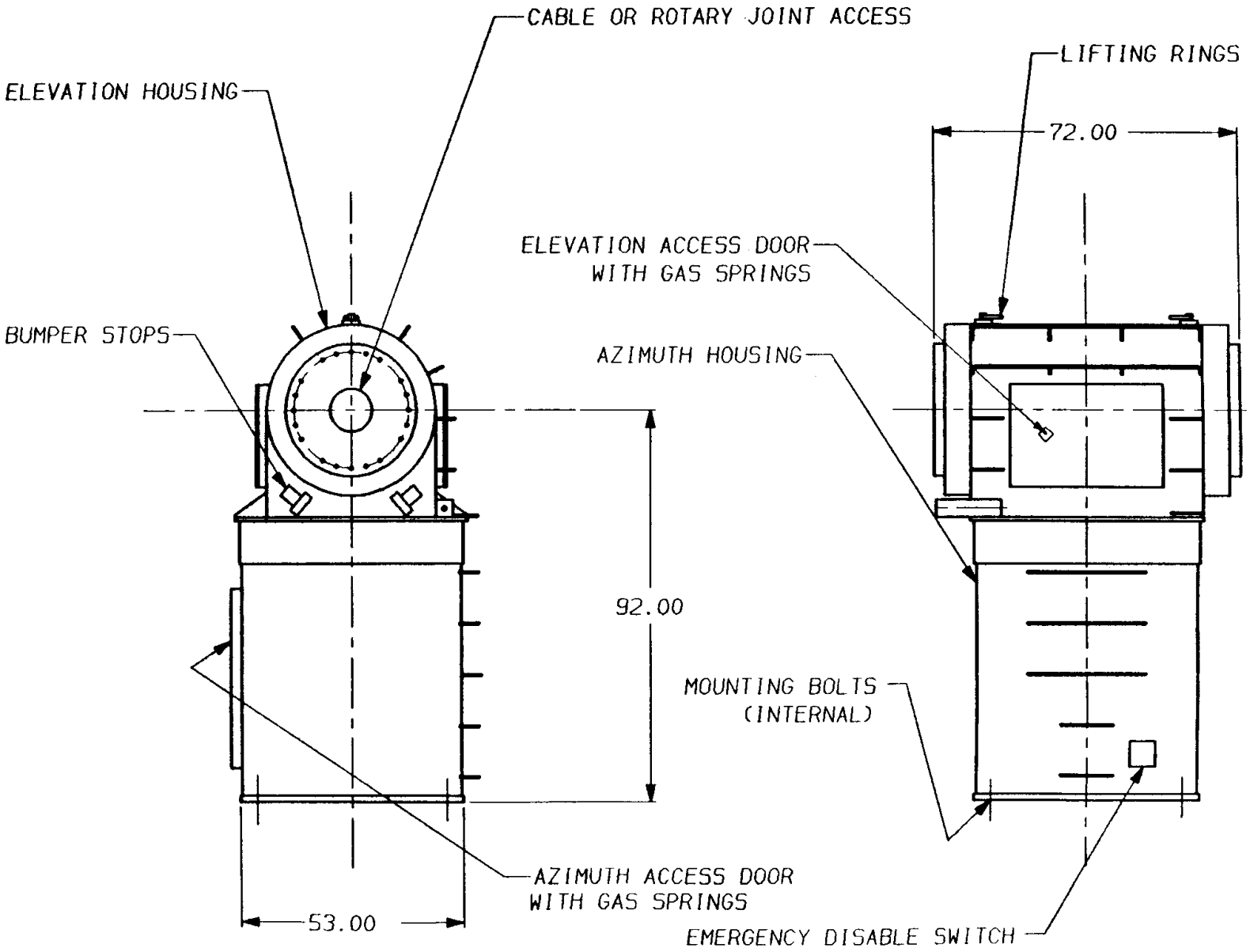

Figure 12. Model 896 Pedestal

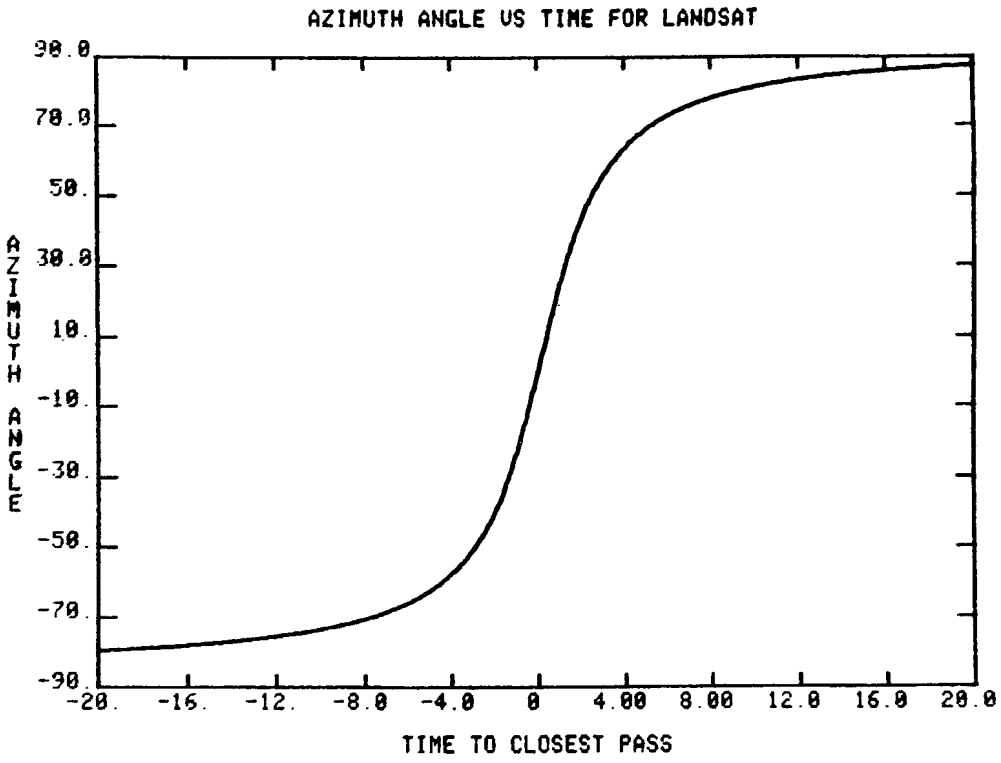

Figure 13. 15 Km Overpass

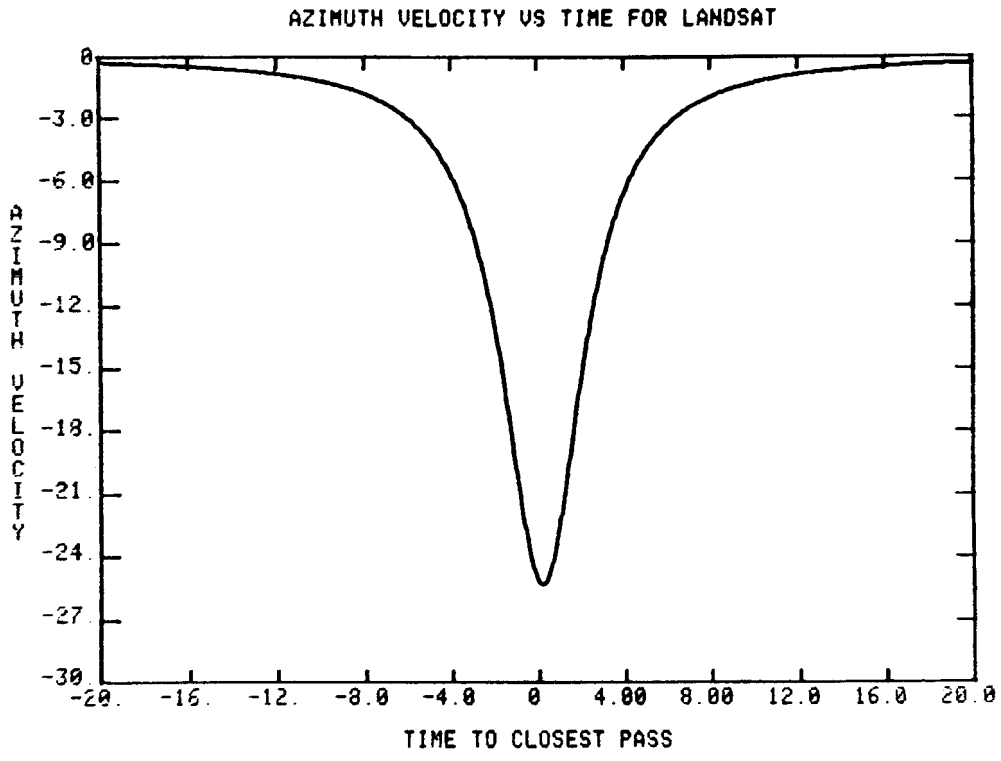

Figure 14. 15 Km Overpass

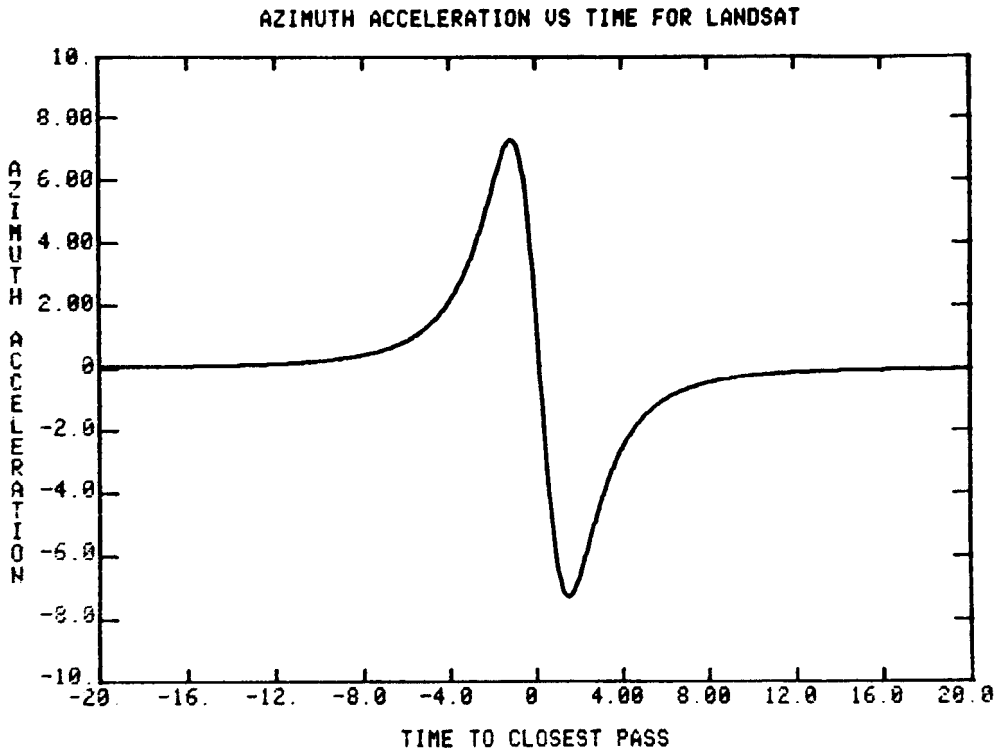

Figure 15. 15 Km Overpass

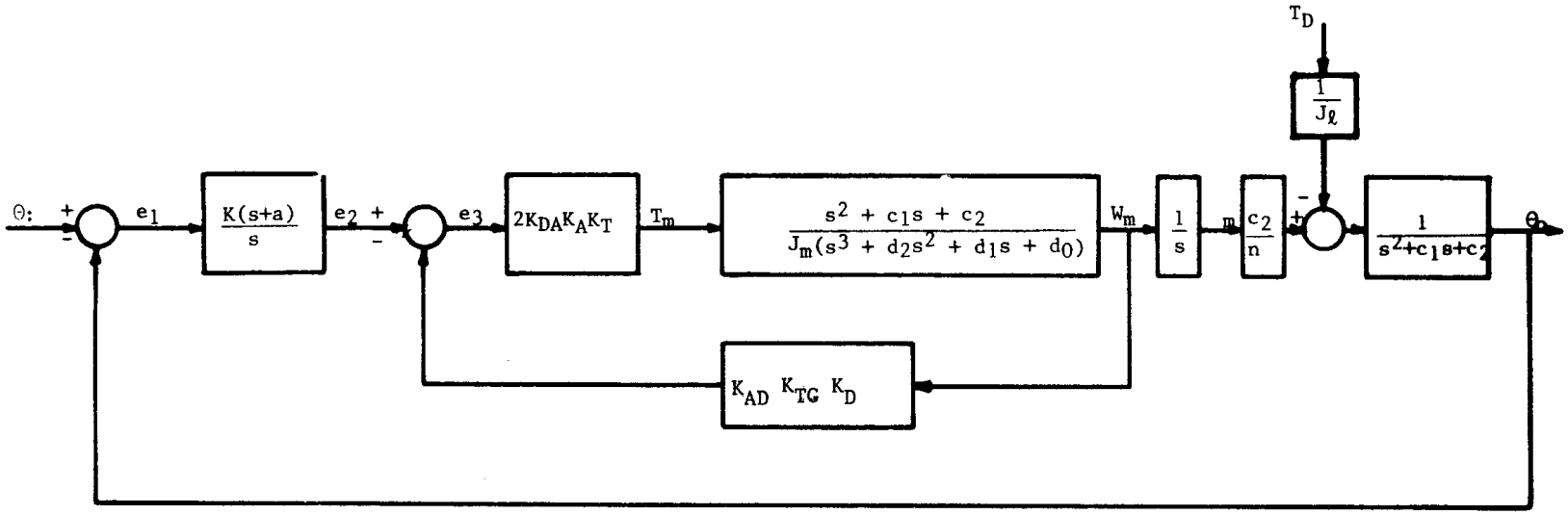

Figure 16. Mathematical Block Diagram of Landsat Control System

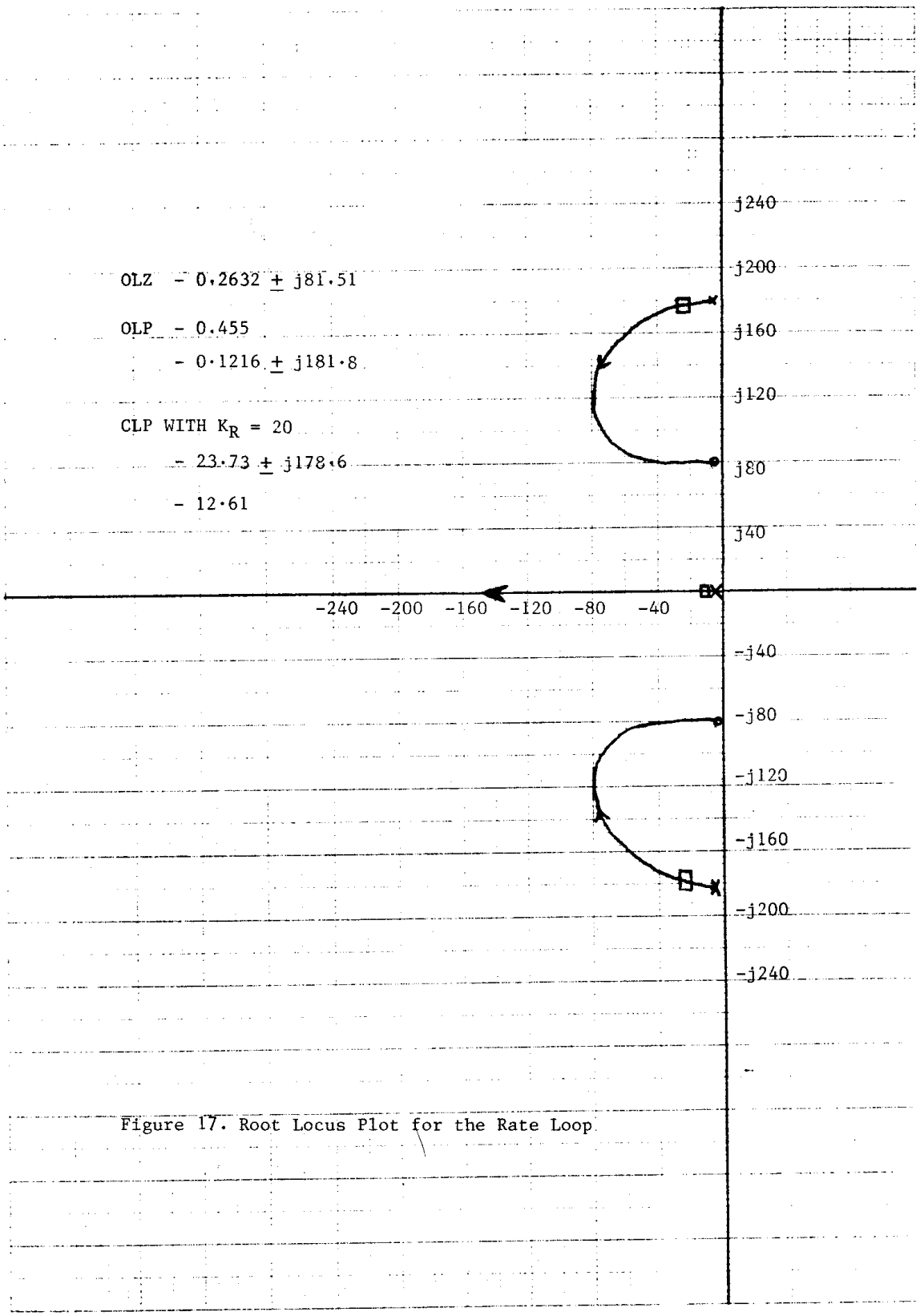

Figure 17. Root Locus Plot for the Rate Loop

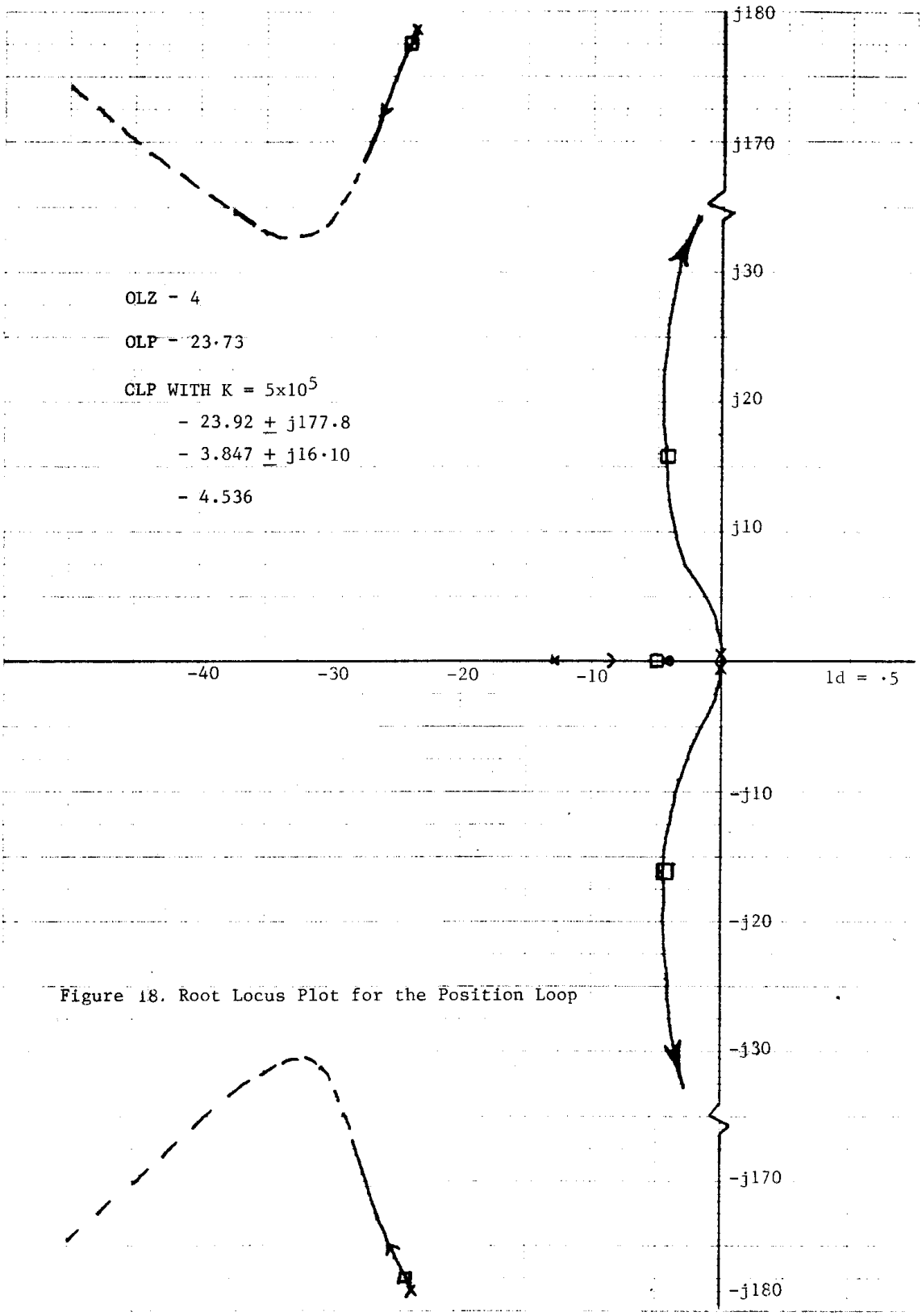

Figure 18. Root Locus Plot for the Position Loop

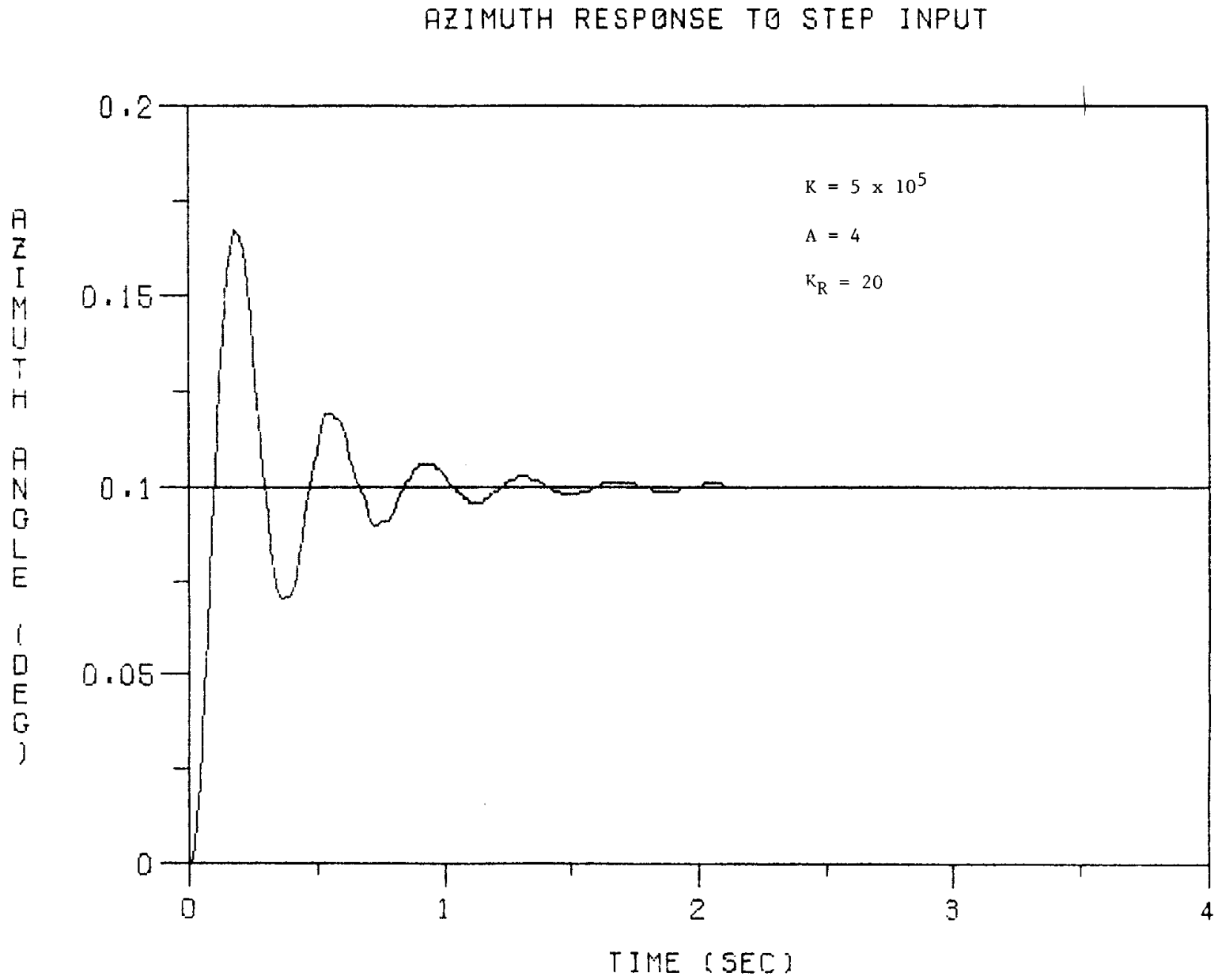

Figure 19. Azimuth Response to Step Input

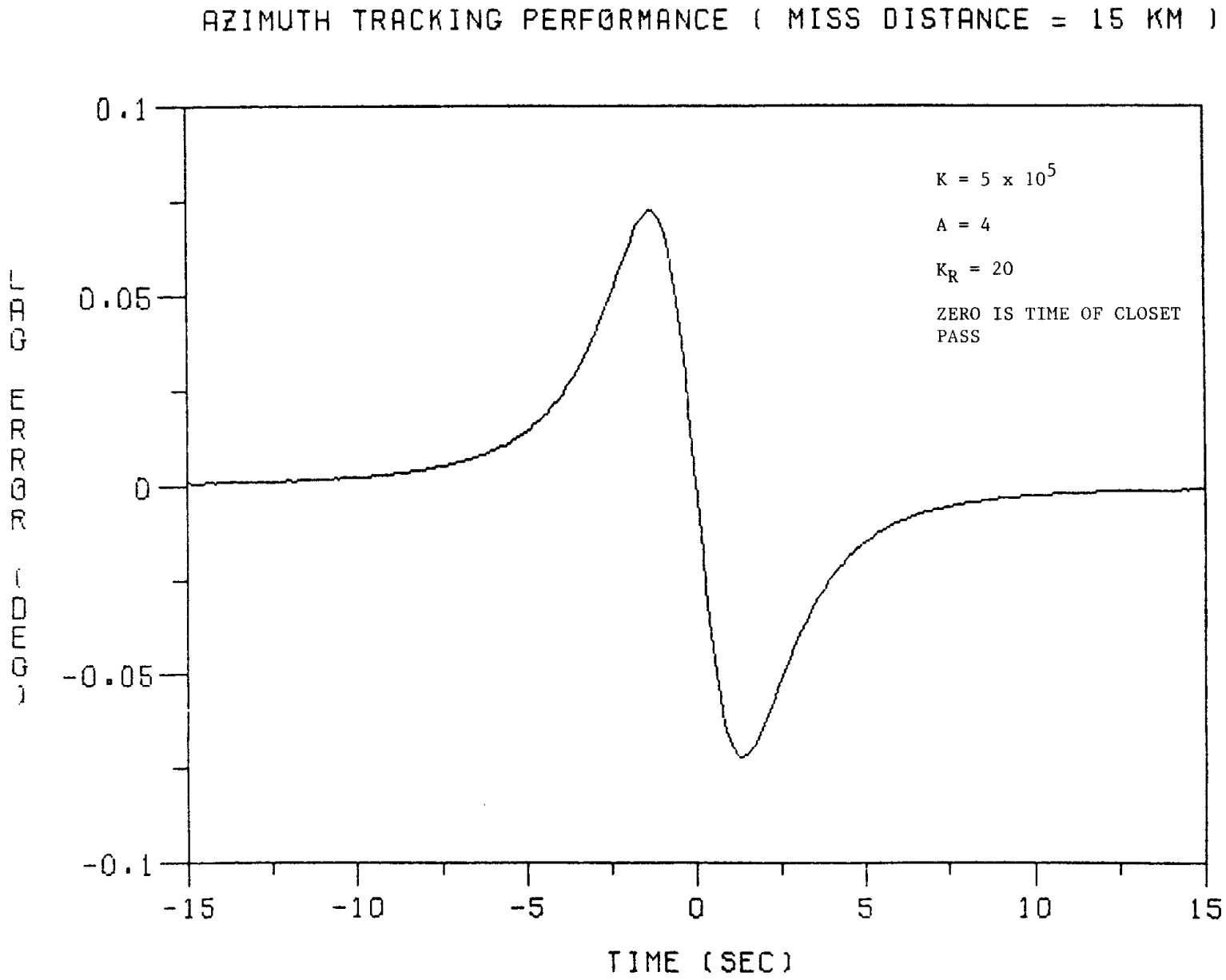

Figure 20. Azimuth Tracking Performance (Miss Distance = 15 Km)

TABLE 1. MAJOR SYSTEM CHARACTERISTICS AND PERFORMANCE

ANTENNA		
TYPE:	DUAL FREQUENCY CASSEGRAIN	
	S-BAND	X-BAND
FREQUENCY (MHz)	2200-2300	8025-8400
CONFIGURATION	SINGLE-CHANNEL MONOPULSE	SINGLE-CHANNEL MONOPULSE
GAIN (dBi) NOMINAL	44.4	55.5
VSWR (MAX)	1.3:1	1.3:1
C/T (dB/°K)(5° ELEVATION)	21.0 AT 2.25 GHz	31.0 AT 8.213 GHz
BEAMWIDTH (NOMINAL)	0.93°	0.25°
POLARIZATION	RHC	RHC
AXIAL RATIO (dB MAX)	1.5	2.0
NULL DEPTH (dB BELOW SUM PEAK, MIN)	25.0	25.0
FIRST SIDELOBE SUPPRESSION (dB BELOW SUM PEAK, MIN)	21.0	21.0
SIZE	10-METER DIAMETER (32.8 FEET)	
FOCAL LENGTH	3.81-METER (12.5 FEET)	
F/D RATIO	0.381	
SURFACE MATERIAL	ALUMINUM SHEET	
SURFACE TOLERANCE	1.14 MM RMS (0.030 INCH)	
SURFACE PANEL CAPS	3.175 MM MAXIMUM (0.125 INCH)	
OPERATING WIND	64 KM/HR (40 MPH) FULL CAPABILITY	
SURVIVAL WIND	160 KM/HR (100 MPH) WHEN IN ZENITH MOUNTING POSITION	
NATURAL RESONANT FREQUENCY	> 5 Hz	
WEIGHT	2210 KILOGRAMS (4872 POUNDS)	
PREAMPLIFIERS		
NOISE FIGURE	0.9 dB 2.2 TO 2.3 GHz 1.6 dB 8.0 TO 8.4 GHz	

GAIN	35 dB 2.2 TO 2.3 GHz 35 dB 8.0 TO 8.4 GHz

DOWNCONVERTERS

INPUT:	S-BAND	X-BAND	X-BAND TRACKING
FREQUENCY	2200 TO 2300 MHz	8.0 TO 8.4 GHz	8.2125 OR 8.253 GHz
IMPEDANCE	50 OHM, COAXIAL	50 OHM, COAXIAL	50 OHM, COAXIAL
NOISE FIGURE	12 dB MAX	15 dB MAX	15 dB MAX
IMAGE REJECTION	>60 dB	>60 dB	>60 dB
SPURIOUS REJECTION	>80 dB	>80 dB	>80 dB
VSWR	1.3:1 MAX	1.2:MAX	1.2:MAX
LOCAL OSCILLATOR:			
FREQUENCY	1970 MHz	7.8275 HGz AND 7.878 GHz	7.9525 CHz
STABILITY	1 x 10^{-9}/SEC 5 x 10^{-8}/HOUR 5 X 10^{-6}/OVER FULL TEMP RANGE	5 x 10^{-6}/OVER FULL TEMP RANGE	5 x 10^{-6}/OVER FULL TEMP RANGE
PHASE NOISE	-120 dB/Hz @ 100 kHz OFFSET	-110 dB/Hz @ 100 kHz OFFSET	-110 dB @ 100 kHz OFFSET
OUTPUT:			
FREQUENCY	230 TO 330 MHz	375 MHz	260 OR 300.5 MHz
IMPEDANCE	50 OHM, COAXIAL	50 OHM, COAXIAL	50 OHM, COAXIAL
MAX OUTPUT LEVEL	+10 dBm	+10 dBm	+10 dBm
RF TO IF GAIN	30 dB NOMINAL	30 dB NOMINAL	20 dB NOMINAL

RECEIVERS

ELECTRICAL:	
RECEIVER TYPE	DOUBLE SUPERHETERODYNE; 60 MHz FIRST IF; 10 MHz SECOND IF
FREQUENCY RANGE	285-410 MHz
INPUT IMPEDANCE	50 OHMS, UNBALANCED
NOISE FIGURE	8.0 dB MAX
VSWR	2:1 MAXIMUM
IMAGE REJECTION	60 dB MINIMUM
IF REJECTION	80 dB MINIMUM
SPURIOUS REJECTION	60 dB MINIMUM
SPURIOUS RADIATION	DESIGNED TO MEET OR EXCEED MIL-STD-461A AND MIL-STD-826A
DYNAMIC RANGE	THRESHOLD TO -10 dBm (THRESHOLD IS DEFINED AS 6 dB SIGNAL-TO-NOISE RATIO IN THE SECOND IF PASSBAND)

LO STABILITY:

VFO	±0.001% PER DEGREE C
CRYSTAL	±0.0005% (0° TO 50°C)

PM (APC) CHARACTERISTICS:

CONTROL RANGE	±250 kHz IN ADDITION TO SECOND LO FINE TUNE RANGE
SEARCH RANGE	50 kHz TO GREATER THAN 500 kHz; APPROXIMATELY SYMMETRICAL ABOUT SECOND LO FREQUENCY SET BY FINE TUNE CONTROL. RANGE SET BY BANDWIDTH CONTROL

PEDESTAL:

VELOCITY	AZ 26°/S EL 5°/S
ACCELERATION CAPABILITY	AZ 10°/S^2 EL 10°/S^2
RATED OUTPUT TORQUE	60,000 FT-LB
SINGLE MOTOR OUTPUT TORQUE	30,000 FT-LB
DRIVE TRAIN COMPLIANCE	4 x 10-8 RAD/FT-LB
AXIS ORTHOGONALITY	0.01 MAX
GEARING TYPE	PLANETARY
GEAR RATIO	AZ-978:1, EL-1676:1
DRIVE, AZIMUTH AND ELEVATION	DUAL BRUSHLESS DC SERVO MOTORS, TORQUE-BIASED
AZIMUTH BEARING DIAMETER	48.0-INCH CROSSED ROLLER
MOTOR ARMATURE INERTIA AT OUTPUT	AZ 3,268 FT-FT-S^2 (ONE MOTOR) EL 9,597 LF-ST-S^2 (ONE MOTOR)
BRAKE ARMATURE AND GEARING INERTIA AT OUTPUT	AZ 4,543 FB-FT-S^2 (ONE MOTOR) EL 13,342 LB-FT-S^2 (ONE MOTOR)
TOTAL INTERNAL INERTIA AT OUTPUT	AZ 15,622 LB-FT-S^2 (TWO MOTORS) EL 45,878 LB-FT-S^2 (TWO MOTORS)
AZIMUTH BEARING OVERTURNING MOMENT CAPACITY	400,000 FT-LB
APPROXIMATE EXTERNAL INERTIA (10-M ANTENNA)	30,000 LB-FT-S^2
BRAKE SIZE	AZ-QTY 2, 26 FT-LB EL-QTY 2, 26 FT-LB

BRAKE TORQUE AT OUTPUT, MINIMUM	50,856 FT-LB
LIMIT STOPS;	
AZIMUTH	PRIMARY ELECTRICAL SECONDARY ELECTRICAL
ELEVATION	PRIMARY ELECTRICAL SECONDARY ELECTRICAL MECHANICAL STOPS
AZIMUTH AXIS CLEARANCE HOLE	10-INCH DIAMETER
ELEVATION AXIS CLEARANCE HOLE	10-INCH DIAMETER
ENVIRONMENT	PEDESTAL AND RISER ARE FULLY SEALED AND CAN BE HEATED OR COOLED TO PROVIDE OPERATION UNDER ANY ATMOSPHERIC AND TEMPERATURE CONDITIONS
STOWING PROVISIONS	HANDCRANKS AND STOW LOCKS
STOW LOCK RATING	EL = 202,000 FT-LB AZ = 102,000 FT-LB
EMERGENCY DISABLE SWITCH	QTY 3 RISER BASE AZIMUTH DRIVE HOUSINC ANTENNA TRUSSWORK
PEDESTAL WEIGHT	12,000 LB
SYSTEM WEIGHT	50,000 LB

X-BAND DEMODULATOR

INPUT SIGNAL:	
CONNECTOR	: N FEMALE
LEVEL	: -10 TO -50 dBm
IMPEDANCE	: 50 OHMS
FREQUENCY	: 375 MHz ± 800 kHz
DATA 1 OUTPUT TM:	
CONNECTOR	: BNC FEMALE
BIT RATE	: 84.9 Mb/s
LEVEL	: ECL
LOAD	: 50 OHMS AT -2 V
DATA 2 OUTPUT MSS:	
CONNECTOR	: BNC FEMALE
BIT RATE	: 15.06 Mb/s
LEVEL	: ECL
LOAD	: 50 OHMS AT -2 V

CLOCK 1 OUTPUT TM CLK:

CONNECTOR	: BNC FEMALE
FREQUENCY	: 84.9 MHz
LEVEL	: ECL
LOAD	: 50 OHMS AT -2 V

CLOCK 2 OUTPUT MSS CLK:

CONNECTOR	: J26 BNC FEMALE
FREQUENCY	: 15.06 MHz
LEVEL	: ECL
LOAD	: 50 OHMS AT -2 V

GENERAL PERFORMANCE:

MODULATION	: UQPSK
BIT RATE	: TM : 84.9 Mb/s
	: MSS : 15.06 Mb/s
BER DEGRADATION	: LESS THAN 2 dB
ACQUISITION TIME	: LESS THAN 300 ms
SEARCH RANGE	: ± 800 kHz, ± 200 kHz, ± 50 kHz, MANUAL

POWER SUPPLY AND CONSUMPTION:

CONNECTOR	:
AC VOLTAGE	: 220 V OR 110 V ± 10%
FREQUENCY	: 47 TO 65 Hz
CONSUMPTION	: 200 W

CONTROL SYSTEM

TYPE : MICROPROCESSOR CONTROLLER

CONTROL MODES:
- AUTOTRACK TYPE I
- AUTOTRACK TYPE II
- POSITION COMMAND
- RATE COMMAND AUTO ACUISITION SCAN
- PROGRAMMED COMMAND

AUTOTRACK TYPE II:
- SERVO BANDWIDTH
- DAMPING RATIO
- ACCELERATION ERROR COEFFICIENT

APPENDIX A

State Variable Model Used in Simulation Program

The following system of state equations represents the dynamics of the continuous plant:

$$\dot{X}_1 = X_2$$

$$\dot{X}_2 = - C_2 X_1 - C_1 X_2 + \frac{C_2}{n} X_3 - \frac{T_c}{J_e}$$

$$\dot{X}_3 = C_2 X_4 + C_1 X_5 + X_6$$

$$\dot{X}_4 = X_5$$

$$\dot{X}_5 = X_6$$

$$\dot{X}_6 = - d_o X_4 - d_1 X_5 - d_2 X_6 + \frac{T_m}{J_m}$$

Where

X_1 = azimuth angle θ_o

X_2 = azimuth rate $\dot{\theta}_o$

X_3 = motor shaft rotation θ_m

X_4, X_5, X_6 = states describing rate loop dynamics

T_c = coulomb friction, $T_c (X_2)$

n = gear ratio

T_m = motor torque

J_m, J_e = motor and antenna load moments of inertia, respectively

The discrete equations describing the microprocessor function are

$$e_1(k) = \theta_i(k) - X_1(k)$$

$$y(k) = y(k-1) + aT\, e_1(k)$$

$$e_2(k) = K\,[y(k) + e_1(k)]$$

$$e_3(k) = e_2(k) - K_R\,[C_2\, X_4(k) + C_1\, X_5(k) + X_6(k)]$$

$$T_m(k) = K_m\, e_3(k), \text{ subject to saturation}$$

where T sampling period

The numerical values of the various parameters pertaining to the Landsat tracking system used in the present analysis are:

$$J_m = 0.01 \text{ lb-ft-s}^2$$

$$J_\ell = 38000 \text{ lb-ft-s}^2$$

$$K_m = 2\, K_{DA}\, K_A\, K_T = 0.02968847 \text{ lb-ft/bit}$$

$$n = 978$$

$$T_c = 2000 \text{ lb-ft}$$

$$C_1 = 0.326 \text{ s}^{-1}$$

$$C_2 = 6644.74 \text{ s}^{-2}$$

$$d_0 = 9749.75 \text{ s}^{-3}$$

$$d_1 = 33043.56 \text{ s}^{-2}$$

$$d_2 = 0.498 \text{ s}^{-1}$$